



University of  
Stavanger

**FACULTY OF SCIENCE AND TECHNOLOGY**

**MASTER'S THESIS**

Study program/ Specialization: Petroleum Engineering/ Reservoir Engineering	Spring semester, 2015  Open
Writer: Farasdaq Muchibbus Sajjad	..... (Writer's signature)
Faculty supervisors: Skule Strand and Tina Puntervold	
Thesis title:  Smart Water EOR Effects in Preserved Sandstone Reservoir Cores, Comparison between Sea Water and Low Salinity Brines at 136°C	
Credits (ECTS): 30	
Key words: EOR Smart Water Low Salinity Sandstone High Temperature Wettability Alteration	Pages : 70 + enclosure : 20  Stavanger, 15 June 2015



**Smart Water EOR Effects in Preserved Sandstone Reservoir Cores,  
Comparison between Sea Water and Low Salinity Brines at 136°C**



---

Universitetet  
i Stavanger

---

**Farasdaq Muchibbus Sajjad**

**University of Stavanger**

**Stavanger, 15 June 2015**

## **ACKNOWLEDGEMENTS**

Researching and studying as a part of Smart Water EOR group at the University of Stavanger truly is one of the best things in my life so far. During my time at the university, I have been surrounded, befriended, and mentored by extremely talented people who show a very deep understanding of their field of expertise. I would like to express my gratitude and appreciation to all those who gave me the possibility to finish my thesis. I would sincerely like to thank Professor Tor Austad, Associate Professor Skule Strand and Postdoctoral Fellow Tina Puntervold for being the best mentors that I could ask for. I could never have made it to see the day that I finish my thesis without their support. They not only showed me how to work, but they showed how to work smartly and taught me how to be an independent researcher. The Smart Water research team has been my academic family during my study and beyond.

Special thanks go to PhD student, Zahra Aghaeifar. She is a great friend that supported and assisted me in my research projects and gave a perspective for working in industry. Also thanks to Aleksandr Mamonov for his assistance and hands on training in the laboratory.

Last but not least, I would like to thank my family and my friends for supporting me in every endeavor.

## ABSTRACT

Low salinity waterflooding is an emerging EOR technique that injects water at significant lower ions concentration as compared to the formation water. Laboratory experiments and field tests show that it can enhance the oil recovery over conventional higher salinity waterflooding. Until now, the mechanism behind low salinity waterflooding is under consideration for further discussions, but it is generally accepted that low salinity waterflooding improves microscopic sweep efficiency by modifying rock wettability. For low salinity condition, it has been suggested that desorption of polar oil components as result of pH increase makes the rock more water-wet.

In this thesis, three coreflood experiments were performed to determine the effect of different water salinities on the oil recovery. Two homogeneous reservoir cores which contain active clays with crude oil which has enough polar organic compounds were used during the experiments. Formation water salinity was 60,461 ppm while the injected brines were modified sea water, (SWm) 30,122 ppm, and modified low salinity brine, (LSm) 1,538 ppm. All experiments were conducted at reservoir temperature, 136°C. Coreflood effluents were sampled regularly to investigate crude oil-brine-rock interactions by measuring pH, density, and different ions concentration of produced water.

The oil recovery factor by using SWm injection was 51% of OOIP. Increased oil recovery was observed during LSm injection, by 12% in the secondary mode (51% compared to 63%), and 9% in the tertiary mode after SWm injection (51% compared to 60%). Also the ultimate recovery was reached much faster using LSm in the secondary mode in comparison to the tertiary mode. The pH increase by performing SWm injection was only 0.4 pH unit while LSm injection resulted in 1.5 pH unit. Even though most experiments in the literature are done at temperature below 100°C, this study shows that there is also a possibility to see low salinity EOR effect at high temperature, up to 136°C.

# TABLE OF CONTENTS

<b>ACKNOWLEDGEMENTS .....</b>	<b>1</b>
<b>ABSTRACT .....</b>	<b>ii</b>
<b>TABLE OF CONTENTS.....</b>	<b>iii</b>
<b>LIST OF FIGURES .....</b>	<b>v</b>
<b>LIST OF TABLES .....</b>	<b>vii</b>
<b>1 INTRODUCTION .....</b>	<b>1</b>
<b>1.1 Introduction .....</b>	<b>1</b>
<b>1.2 Thesis Objective.....</b>	<b>2</b>
<b>2 BASIC RESERVOIR ENGINEERING OVERVIEW .....</b>	<b>3</b>
<b>2.1 Sedimentology and Mineralogy .....</b>	<b>3</b>
2.1.1 Sandstone .....	3
2.1.2 Clay.....	5
<b>2.2 Hydrocarbon Recovery Mechanism .....</b>	<b>8</b>
2.2.1 Primary Recovery .....	8
2.2.2 Secondary Recovery .....	8
2.2.3 Tertiary Recovery .....	9
<b>2.3 Displacement forces.....</b>	<b>12</b>
2.3.1 Capillary forces.....	12
2.3.2 Viscous forces .....	13
2.3.3 Gravitational Forces .....	14
<b>2.4 Wettability .....</b>	<b>14</b>
2.4.1 Wettability Measurement.....	15
2.4.2 Wettability Impact on Oil Recovery .....	17
<b>3 SMART WATERFLOODING .....</b>	<b>18</b>
<b>3.1 Low Salinity History .....</b>	<b>18</b>
<b>3.2 Condition For Low Salinity Effects.....</b>	<b>19</b>
<b>3.3 Wettability Alteration .....</b>	<b>20</b>
<b>3.4 Suggested Low Salinity EOR Mechanism .....</b>	<b>23</b>
3.4.1 Migration of Fines .....	23
3.4.2 pH Increase .....	24
3.4.3 Multi Ion Exchange.....	25
3.4.4 Double Layer Effect .....	26
3.4.5 Salting-in Effect .....	26
3.4.6 Desorption by pH Increase .....	27
<b>3.5 Laboratory and Field Case Study.....</b>	<b>29</b>
3.5.1 Relative Permeability .....	29
3.5.2 Outcrop versus Reservoir Cores.....	29
3.5.3 Mineralogy .....	30
<b>4 EXPERIMENTAL WORK .....</b>	<b>32</b>
<b>4.1 Experimental Material .....</b>	<b>32</b>
4.1.1 Core.....	32
4.1.2 Crude Oil .....	32
4.1.3 Brine.....	33
<b>4.2 Experiment Steps.....</b>	<b>34</b>
4.2.1 Brines and Oil Preparation .....	34
4.2.2 Core Cleaning .....	36

4.2.3	Permeability Measurement .....	38
4.2.4	Fluid Saturation.....	38
4.2.5	Aging of Core.....	41
4.2.6	Oil Recovery Test.....	42
4.2.7	Effluent Collection.....	43
<b>5</b>	<b>RESULTS .....</b>	<b>46</b>
<b>5.1</b>	<b>Oil Recovery Test on Core-3, 1<sup>st</sup> Restoration .....</b>	<b>46</b>
<b>5.2</b>	<b>Oil Recovery Test on Core-3, 2<sup>nd</sup> Restoration.....</b>	<b>49</b>
<b>5.3</b>	<b>Oil Recovery Test on Core-5, 1<sup>st</sup> Restoration .....</b>	<b>53</b>
<b>6</b>	<b>DISCUSSION.....</b>	<b>58</b>
<b>6.1</b>	<b>Oil Recovery .....</b>	<b>58</b>
<b>6.2</b>	<b>pH Analysis.....</b>	<b>60</b>
<b>6.3</b>	<b>Ion Chromatography Analysis.....</b>	<b>62</b>
6.3.1	Calcium.....	62
6.3.2	Magnesium .....	63
6.3.3	Sulfate .....	63
<b>6.4</b>	<b>pH Screening Test .....</b>	<b>64</b>
<b>6.5</b>	<b>Temperature and Formation Water Salinity Effect .....</b>	<b>65</b>
<b>6.6</b>	<b>Viability of Smart Water Fluids .....</b>	<b>67</b>
<b>7</b>	<b>CONCLUSION .....</b>	<b>69</b>
<b>8</b>	<b>FUTURE WORK.....</b>	<b>70</b>
	<b>REFERENCES .....</b>	<b>71</b>
	<b>SYMBOLS AND ABBREVIATIONS .....</b>	<b>75</b>
	<b>APPENDICES .....</b>	<b>77</b>
<b>A.1</b>	<b>AN and BN Measurement .....</b>	<b>77</b>
<b>A.2</b>	<b>Viscosity Measurement .....</b>	<b>77</b>
<b>A.3</b>	<b>Ion Chromatography.....</b>	<b>78</b>

## LIST OF FIGURES

Figure 1. Statistical relationship between porosity and depth over 30,122 sandstone reservoirs around the world. Redrawn from Nadeau et al <sup>7</sup> .....	4
Figure 2. Statistical relationship between porosity and permeability over 30,122 sandstone reservoirs around the world. Redrawn from Nadeau et al <sup>7</sup> .....	5
Figure 3. Structure of a tetrahedral and octahedral layer. Redrawn from IDF <sup>8</sup> .....	6
Figure 4. Mineralogy structure in different type of clays. Redrawn from Morad et al. <sup>9</sup> .	8
Figure 5. Design and implementation steps of a comprehensive EOR project <sup>14</sup> .....	9
Figure 6. Macroscopic/volumetric sweep efficiency illustration (areal and vertical) ....	11
Figure 7. Fluid distribution in wetting condition .....	15
Figure 8. Contact angle wettability measurement illustration .....	16
Figure 9. Initial wetting distribution over 32 sandstone reservoirs. Data is taken from Treiber et al <sup>17</sup> .....	17
Figure 10. Residual oil saturation vs Amott Harvey Wettability Index. Adapted from Skauge <sup>18</sup> (a) and Oil Recovery vs wetting conditions. Adapted from Strand <sup>16</sup> (b).....	17
Figure 11. Wettability alteration in low salinity waterflooding (adapted from Strand and Puntervold <sup>30</sup> ) .....	20
Figure 12. Detachment of clay particles and mobilization of oil.Redrawn from Tang <sup>35</sup>	24
Figure 13. MIE mechanism illustration. Redrawn from Lager et al. <sup>38</sup> .....	26
Figure 14. Salting out and salting in mechanism illustrations <sup>41</sup> .....	27
Figure 15. Proposed mechanism for acidic and basic organic material desorption from clay surface during low salinity flooding, Redrawn from Austad et al <sup>3</sup> .....	28
Figure 16. Adsorption of quinoline versus pH at ambient temperature in low salinity brine, LS (1,000 ppm), and in high salinity brine, HS (25,000 ppm). The dashed line represents the pKa value of quinoline (4.9). Redrawn from Aksulu et al. <sup>42</sup> .....	29
Figure 17. Incremental oil recovery from outcrop cores and reservoir cores. Redrawn from Winoto et al. <sup>44</sup> .....	30
Figure 18. Core-5 captured from different angle .....	32
Figure 19. Schematic drawing of experiment steps .....	34
Figure 20. Viscous flooding experiment steps.....	34
Figure 21. Water filtration setup illustration .....	35
Figure 22. Measurement of AN and BN by a titrator .....	36
Figure 23. Viscosity measurement by a spectrometer.....	36
Figure 24. Effluents from kerosene cleaning.....	37
Figure 25. Schematic of equipment used for diluted formation water saturation to the core .....	39
Figure 26. Desiccator illustration.....	40
Figure 27. Oil saturation setup illustration.....	41
Figure 28. Oil recovery test setup illustration .....	42
Figure 29. Mettler Toledo Seven Easy pH instrument .....	44

Figure 30. Gilson GX-271 Liquid Handle (a) and Dionex ICS-3000 Ion Chromatography (b)	45
Figure 31. Antoon Paar 4500 Density Meter	45
Figure 32. Oil recovery during the 1 <sup>st</sup> restoration of core-3	47
Figure 33. Pressure drop and temperature across the core during oil recovery test on core-3 (1 <sup>st</sup> restoration)	48
Figure 34. Produced water pH and density during oil recovery test on core-3 (1 <sup>st</sup> restoration)	48
Figure 35. Ion chromatography analysis during oil recovery test on core-3 (1 <sup>st</sup> restoration)	49
Figure 36. Oil recovery during the 2 <sup>nd</sup> restoration of core-3	50
Figure 37. Pressure drop and temperature across the core during oil recovery test on core-3 (2 <sup>nd</sup> restoration)	51
Figure 38. Produced water pH and density during oil recovery test on core-3 (2 <sup>nd</sup> restoration)	52
Figure 39. Ion chromatography analysis during oil recovery test on core-3 (2 <sup>nd</sup> restoration)	53
Figure 40. Oil recovery during 1 <sup>st</sup> restoration of core-5	54
Figure 41. Pressure drop and temperature across the core during oil recovery test on core-5 (1 <sup>st</sup> restoration)	55
Figure 42. Produced water pH and density during oil recovery test on core-5 (1 <sup>st</sup> restoration)	56
Figure 43. Ion chromatography analysis during oil recovery test on core-5 (1 <sup>st</sup> restoration)	57
Figure 44. Comparison oil recovery for all experiments	599
Figure 45. pH screening test of core-4 at 136°C <sup>48</sup>	65
Figure 46. Macroscopic/volumetric sweep efficiency illustration (areal and vertical) in a three-dimensional model	68
Figure A-1. Flowchart of Ion Chromatography experiment	78
Figure A-2. The position of the samples in the sampler of IC system	79
Figure A-3. The containers of anion and cation eluent DI water	79
Figure A-4. An example of the list of sample data, containing their names and positions in the sampler	80
Figure A-5. Venting the air from pumps	80
Figure A-6. Preparing the instruments in the program of the IC software for (a) Anion and (b) Cation	81
Figure A-7. Adding and starting the measurement in IC system	82
Figure A-8. Analyzing the obtained result after IC measurements	83

## LIST OF TABLES

Table 1. Properties Clay Minerals <sup>8</sup> .....	7
Table 2. Contact angle and wettability preference <sup>6</sup> .....	16
Table 3. Mechanisms of organic matter adsorption onto clay mineral .....	25
Table 4. Physical core data .....	33
Table 5. Oil properties .....	33
Table 6. Chemical composition of brines .....	33
Table 7. Breakthrough time and oil recovery for all experiments .....	59

# 1 INTRODUCTION

## 1.1 Introduction

The majority of the current world oil production originates from developed fields, and therefore expanding oil recovery becomes critical. This situation agrees with the growth of world energy demand up to 37% for two decades later<sup>1</sup>. Along these lines, it becomes crucial to increase recovery factor from developed fields as well as for new fields through secondary and tertiary production phase to overcome the energy needs in the future.

Waterflooding as the most common secondary recovery method are usually used for pressure maintenance and physically sweep oil in the reservoir. In the conventional waterflooding the injected water may be taken from the nearest sources: produced formation water or sea water. From a conventional point of view, the injection brine composition and ions were believed to have no effect on the recovery efficiency during waterflooding process.<sup>2</sup> However, over the last decade, several laboratory studies and field tests have shown low salinity/smart waterflooding improved oil recovery compare to high salinity waterflooding for sandstone reservoir. The technique is applied by injecting water at significantly lower salinity compared to salinity of formation water.

Until now, the mechanisms behind low salinity waterflooding is under consideration for further discussions, but it is generally accepted that the purpose of low salinity waterflooding is to improve microscopic sweep efficiency by modifying rock wettability. For low salinity condition, Austad et.al<sup>3</sup> suggest that desorption of polar oil components by pH increase makes the rock more water-wet. Therefore it can affect the oil recovery which depends on polar components in the crude oil, divalent cations in the formation brine, and active clays in the sandstone.

It is important to conduct further research about low salinity water as an affordable EOR method. In addition, low salinity brine does not need hazardous chemical; its result is an environmentally friendly EOR. This method can be applied for current or planned waterflooding projects, both offshore and onshore field location. Problems associated with conventional waterflooding, such as scale formation, souring, and filtration at the ion levels can be mitigated with low salinity waterflooding method.

## 1.2 Thesis Objective

This thesis is related to an actual company project and during the experiment reservoir cores were used. The main objectives of this thesis are:

1. To compare smart waterflooding performance in a high temperature sandstone reservoir (136°C), by using modified sea water (30,122 ppm) and modified low salinity water (1,538 ppm) which both have lower salinity than formation water (60,461 ppm). The low salinity waterflooding process will be performed in secondary and tertiary injection mode.
2. To validate low salinity waterflooding mechanism that has been proposed by Austad et.al<sup>3</sup> with regards to desorption of polar component of the crude oil by pH increase.

## **2 BASIC RESERVOIR ENGINEERING OVERVIEW**

### **2.1 Sedimentology and Mineralogy**

Sedimentary rock is mainly generated by huge accumulation of clastic sediments in aqueous environment such as river channels, deltas, beaches, lakes and submarine fans. By the above accumulation condition, sediments are mostly water-wet by nature.<sup>4</sup>

#### **2.1.1 Sandstone**

Sandstone is a sedimentary rock which has grain size ranging from 62  $\mu\text{m}$ -2 mm. The mineral composition of the grain varies, but usually consists of mainly quartz ( $\text{SiO}_2$ ) with limited amounts of feldspar, mica, biogenic particles, and many other mineral species. High silica content is always observed in sandstones, that's why they are often referred as siliciclastic rocks.

Sandstone reservoirs contribute to 50% of oil reserves in the world.<sup>5</sup> It is most commonly found unfractured, so that possibility of unswept oil in the matrix blocks can be avoided. By having the above qualities, sandstone reservoirs are generally excellent candidate for waterflooding.

##### **2.1.1.1 Porosity**

Porosity is ratio of void volume to the total rock volume. This volume is unoccupied by grains and minerals, and therefore can hold and transport fluids. There are effective porosity and total porosity. Effective porosity accounts for connected pore space in the rock, while total porosity accounts for total pore space in the rock. It means that effective porosity is always smaller than total porosity. There are several factors that control effective porosity: rock type, grain size, grain packing and orientation, cementation, weathering, leaching, as well as the type, content, and hydration of clay minerals.<sup>6</sup>

Porosity may also be classified based on its origin from geological process, either as primary porosity or secondary porosity. Primary porosity is the porosity which developed during sedimentary deposition. Secondary porosity exists after primary porosity by alteration of rock, commonly through processes such as dissolution, fracturing, and dolomitization.

### 2.1.1.2 Permeability

Permeability is the measurement of a rock's ability to transmit fluid with given differential pressure, cross-sectional area and fluid viscosity. It means that higher permeability represents lower fluid flow resistance in the reservoir. The absolute permeability represents as a constant property of the porous medium when a single fluid flows through the porous medium. When two or more phases occur, the rock's permeability is different from single phase condition. Relative permeability for each phase is depending on total permeability, saturation and viscosity of each phase, and capillary pressure between phases.

Porosity and permeability properties are usually dependent on each other, and vary with depth. When the depth increases, the impact of overburden pressure to the unit volume of rock also increases. It could increase compaction, decrease pore space and reduce rock's permeability. Nadeu et al.<sup>7</sup> did extensive research between porosity, permeability, and reservoir depth around the world as shown on Figure 1 and Figure 2.

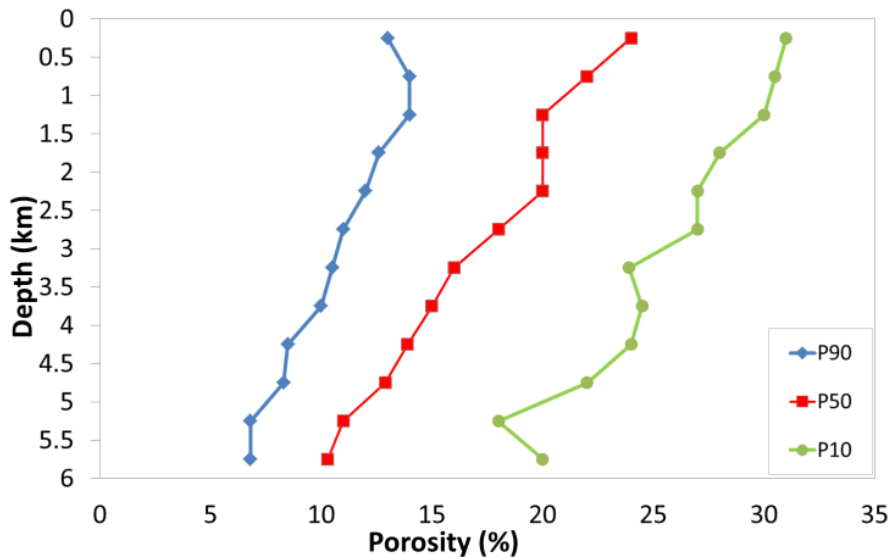


Figure 1. Statistical relationship between porosity and depth over 30,122 sandstone reservoirs around the world. Redrawn from Nadeu et al<sup>7</sup>

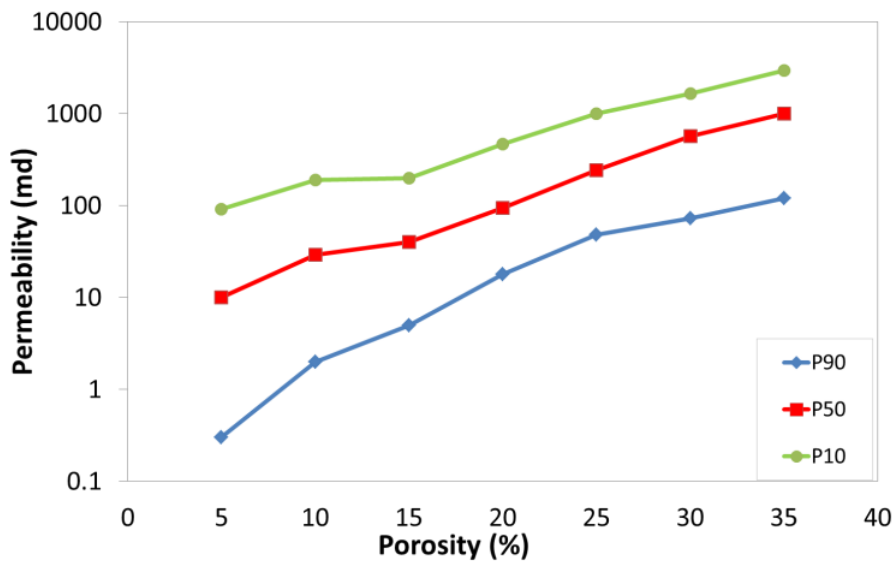


Figure 2. Statistical relationship between porosity and permeability over 30,122 sandstone reservoirs around the world. Redrawn from Nadeau et al<sup>7</sup>

### 2.1.2 Clay

Clay can be described chemically as aluminium silicates. The essential mineral composition consists of silica (Si), alumina (Al) and water. The frequently appeared elements are Iron (Fe) and magnesium (Mg), and also smaller quantities of sodium (Na) and potassium (K). Clay typical properties are fine size, large surface area, cation exchange capacity, and chemical reactivity of the surface.<sup>8</sup>

Every sandstone reservoir contains a certain amount of clay in the formation. Clay content in sandstone reservoir will degrade the reservoir quality since it will increase the irreducible water saturation and also can reduce the permeability of the reservoir greatly. However, in low salinity waterflooding the clay presence is essential to achieve the optimum result for enhanced oil recovery. Sandstone reservoir clays are commonly made up of sheets of tetrahedral silica and octahedral aluminium layers, as illustrated in Figure 3.

Cation Exchange Capacity (CEC) is an important property of clay which describes the total capacity of a clay surface to attract and hold exchangeable cations. It is commonly expressed in millequivalents of cation per 100 grams of clay (meq/100g). The imbalance of structural charge, either in the silica or in the aluminium layer and also at the edge surfaces, will cause to have a negative charge on the clay surface.<sup>3</sup> Cations will adsorb onto these negatively charged sites of the clay surface, where weak bonds can be

established. As a result of these weak bonds, cations can readily be exchanged with other cations. Due to the clay's ability to exchange cations adsorbed to the external surfaces and between the layers of the clay structure, it is common to refer clay minerals as cation exchange materials. The replacing power of the different cations in solution often referred as the relative affinity of those cations to the clay surface, which is believed at the room temperature condition to be;

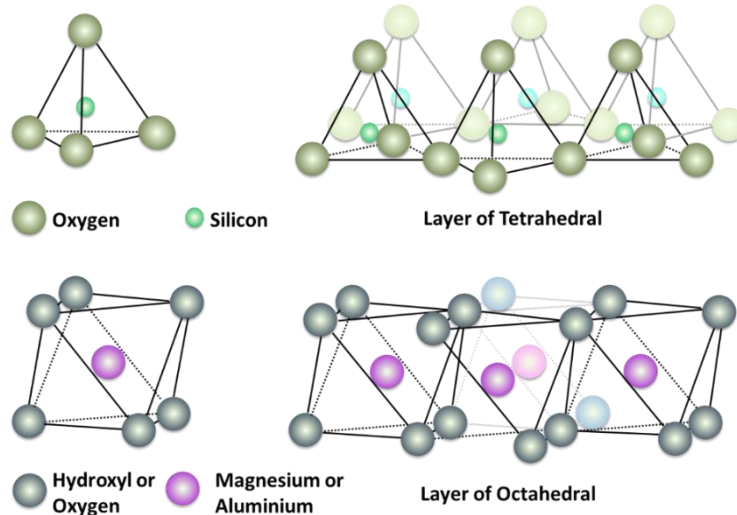


**Figure 3. Structure of a tetrahedral and octahedral layer. Redrawn from IDF<sup>8</sup>**

The replacing power also depends on relative concentration of the different cations. Lower replacing power cations can still replace ions with higher affinity if the relative concentration is high enough. It is noticed that hydrogen,  $\text{H}^+$ , has the highest affinity, even at a very low concentration,  $10^{-8}$  mole/liter i.e.  $\text{pH} = 8$ , is still reactive towards the clay surface.

There are four different type of clay, kaolinite, illite, chlorite, and montmorillonite. The clays different properties are described below:

- Kaolinite is regarded as a non-swelling clay. It is characterized as 1:1 clay, meaning that one unit consist of one tetrahedral silica layer and one alumina layer, and the unit are bonded together by strong hydrogen bonds.<sup>9</sup> This clay has a relative low cation exchange capacity due to the well balanced charges within the kaolinite structure. The clay has a trend of transforming into illite and chlorite in proportion of depth, mostly in very deep formation. Tang and Morrow<sup>10</sup>, was the first to suggest that one of the proposed mechanisms the presence of clays or potentially mobile fines in low salinity water flooding. Later, a relationship suggesting that additional oil recovery was directly proportional to the kaolinite content in the rock was put forward by Jerauld et

al.<sup>11</sup> Positive results in kaolinite-free sandstone samples after low salinity injection was seen after a recent work done by Bousseour et al.<sup>12</sup>

- Illite and mica are regarded as non-swelling clay. They are characterized as a 2:1 clay, and one unit consist of three sheets where the octahedral alumina layer lies between two tetrahedral silica layers. The charge imbalance is mostly located in the silica layers ( $\text{Si}^{4+}$  is substituted by  $\text{Al}^{3+}$ ), which creates a negatively charge surface. Illite and mica is differentiated only by the degree of charge imbalance in the silica layers that resulted on a lower negative surface charge on illite compared to mica. Illite is a non-swelling clay. the CEC and the surface area are much larger than kaolinite.<sup>9</sup>
- Montmorillonite has a similar structure as illite/mica, i.e. It is 2:1 clay. However, the charge imbalance is mostly located in the alumina layer ( $\text{Al}^{3+}$  is substituted by  $\text{Mg}^{2+}$ ). Montmorillonite cation exchange capacity is very high, but it has a tendency to swell greatly due to large distance between the cations and the negatively charge alumina layer.<sup>9</sup>
- Chlorite has a 2:1:1 structure comprised of a negatively charge 2:1 tetrahedral-octahedral-tetrahedral layered structure inter-layered with an additional octahedral layer that is positively charged and composed of cations and hydroxyl ions. Cation exchange capacity is in the same range as for illite/mica, however it has very large surface area. The swelling degree of chlorite is low.<sup>9</sup>

Clay properties are summarized in Table 1. Figure 4 illustrates the structure of each clay type. Regarding low salinity waterflooding, illite and kaolinite are the desirable type of clays due to their cation exchange capacity and non swelling clay.

**Table 1. Properties Clay Minerals<sup>8</sup>**

Property	Kaolinite	Illite/Mica	Montmorillonite	Chloride
Layers	1:1	2:1	2:1	2:1:1
Particle Size (micron)	5-0.5	Large sheets to 0.5	2-0.1	5-0.1
CEC (meq/100g)	3-15	10-40	80-150	10-40
Surface Area BET-N <sub>2</sub> (m <sup>2</sup> /g)	15-25	50-110	30-80	140

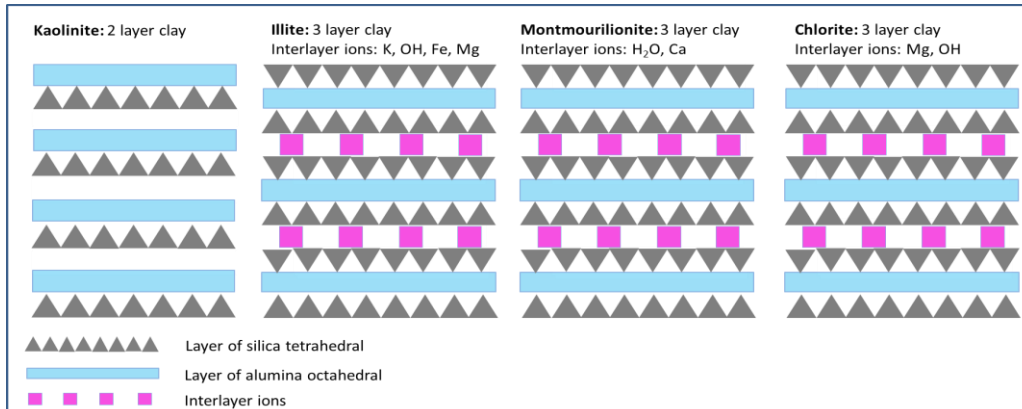


Figure 4. Mineralogy structure in different type of clays. Redrawn from Morad et al.<sup>9</sup>

## 2.2 Hydrocarbon Recovery Mechanism

Hydrocarbon recovery mechanism has been divided into three stages which are primary, secondary and tertiary recovery. In many situations, oil recovery mechanism is not conducted with the specific order. In modern field development, secondary and tertiary recovery methods are sometimes conducted at early stage of production. Therefore the term tertiary recovery is replaced by more accepted term “Enhanced Oil Recovery” (EOR).

### 2.2.1 Primary Recovery

Primary recovery mechanism is the initial production stage that rely-on natural energy present in the reservoir. Primary recovery is the initial production of reservoir that resulting from simple pressure depletion where the only reservoir energy is used to produce the oil. The energy sources are solution gas drive, gas cap drive, water drive, fluid and rock expansion and gravity drainage. This means that the reservoir pressure is used to produce fluids out of the reservoir. Primary recovery mechanism also includes artificial lift such as gas lift and electrical submersible pump. The recovery factor of primary recovery mechanisms are relatively low, ranging from 5% to 30% of original oil in place.<sup>13</sup>

### 2.2.2 Secondary Recovery

Secondary recovery mechanism is usually implemented when the energy drive from the reservoir is depleted. The reservoir pressure will decline until it could not maintain

production of hydrocarbon. Since there is not enough energy in the reservoir to produce hydrocarbon, it needs to supply energy from the surface. Usually secondary recovery mechanism is by injecting fluids into reservoir for pressure maintenance and displacement of oil. Pressure maintenance includes water injection, gas injection and water alternating gas injection. The most applied pressure maintenance is waterflood. The recovery factor for reservoirs that have conducted waterflood could reach 35% to 50% of the original oil in place.<sup>13</sup>

### 2.2.3 Tertiary Recovery

When the secondary recovery phase reaches the economical limit, there is still a significant volume of oil left in the unswept part and residual oil of the reservoir. The overall objective of tertiary recovery/EOR processes is to enhance the overall oil displacement efficiency in the reservoir. There are several steps in the EOR project plan and execution as shown in Figure 5.

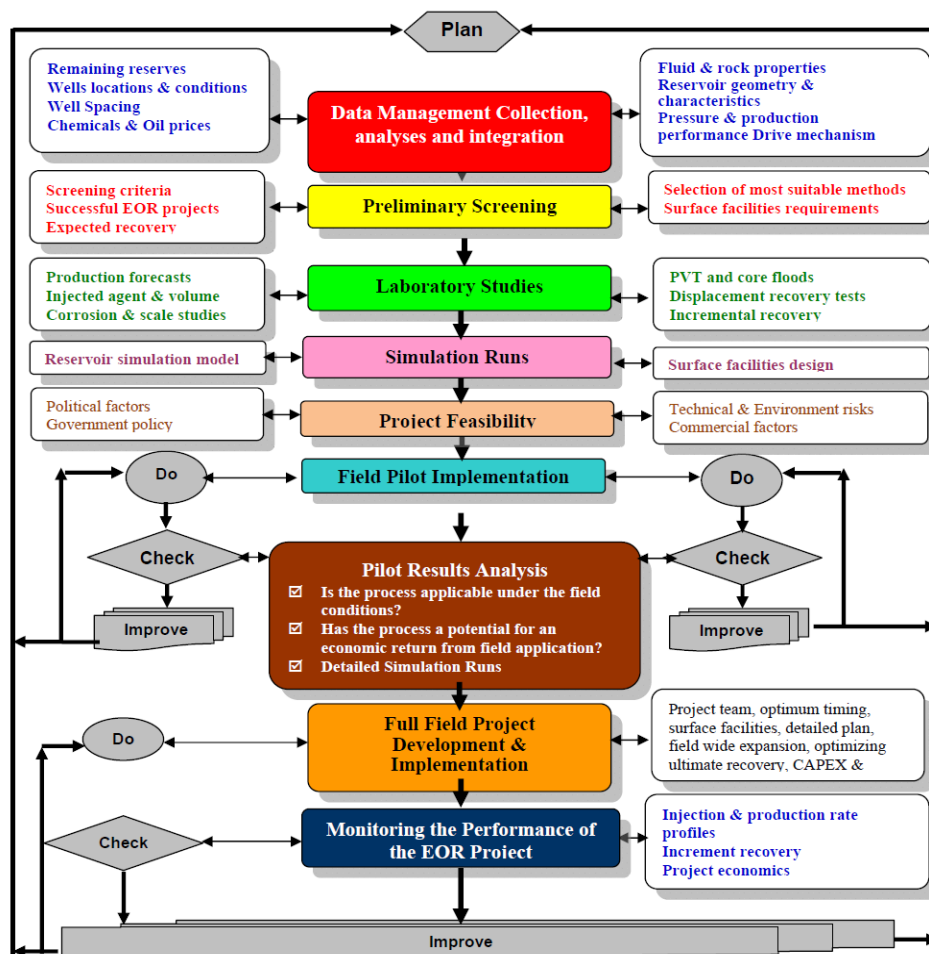


Figure 5. Design and implementation steps of a comprehensive EOR project<sup>14</sup>

### 2.2.3.1 Displacement Efficiency

Displacement efficiency is a function of microscopic and macroscopic displacement efficiency. Microscopic sweep efficiency means the displacement or mobilization of oil at pore scale, and represents the effectiveness of displacing fluid contacts the oil. Wettability has great influence on microscopic efficiency. Equation 1 is the formula of microscopic sweep efficiency.<sup>13</sup> In general, elevating the microscopic sweep efficiency can be done by lowering capillary forces.

$$E_d = \frac{1 - S_{iw} - S_{or}}{1 - S_{iw}} \quad (1)$$

Where

$E_d$  : Microscopic sweep efficiency

$S_{iw}$  : Initial water saturation

$S_{or}$  : Residual oil saturation

Macroscopic sweep efficiency depends on the effectiveness of the displacing fluid in contacting the reservoir in taking out the volume of reservoir, both areally and vertically. Macroscopic sweep efficiency is controlled mainly by mobility ratio. Mobility ratio is defined as the ratio of the mobility between displacing fluid and displaced fluid. In the waterflooding process oil is the displaced fluid and water the displacing fluid as shown in equation 2.<sup>13</sup> When mobility ratio is bigger than 1, it creates an unstable displacement process which may create viscous fingering. So that to have high macroscopic sweep efficiency the mobility ratio should be less than 1. Figure 6 illustrates the macroscopic sweep efficiency in the waterflooding process.

$$M = \frac{k_{rw} \cdot \mu_o}{k_{ro} \cdot \mu_w} \quad (2)$$

Where

$k_{rw}$  : Relative permeability of the water

$k_{ro}$  : Relative permeability of the oil

$\mu_w$  : Water viscosity

$\mu_o$  : Oil viscosity

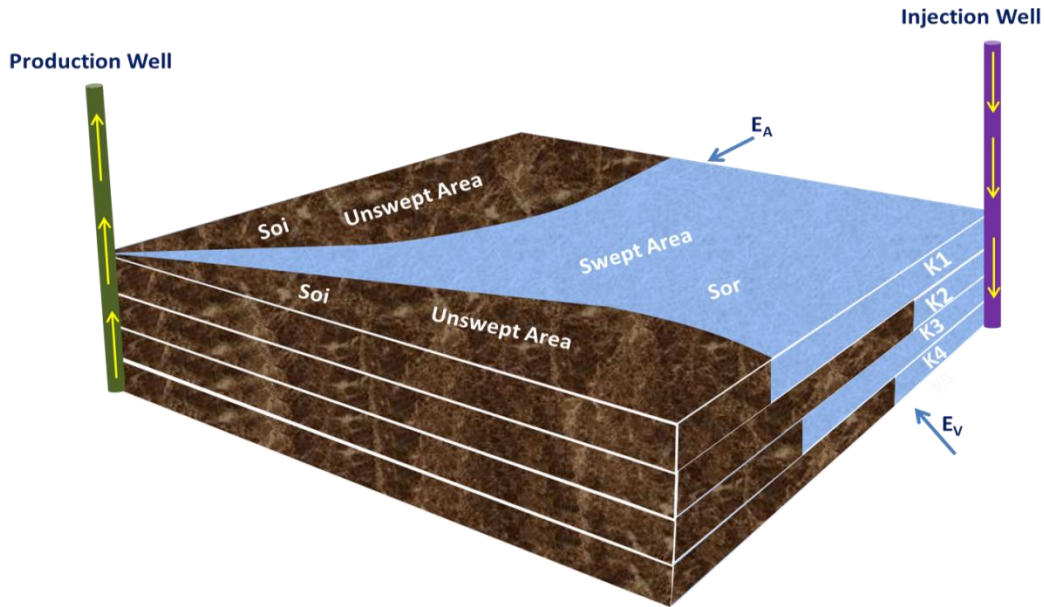


**Figure 6. Macroscopic/volumetric sweep efficiency illustration (areally and vertically)**

The total displacement efficiency ( $E_T$ ) then is the product of microscopic sweep efficiency ( $E_d$ ) and the macroscopic sweep efficiency ( $E_M$ ) as shown in the following equation.<sup>13</sup>

$$E_T = E_d \times E_M \quad (3)$$

### 2.2.3.2 Type of EOR Methods

EOR process may involve injection of miscible gases, chemicals and thermal energy into the reservoir to displace additional oil. For miscible process the objective is to inject fluids that are miscible with the oil in the reservoir through composition alteration, for example, injection of solvents or  $CO_2$ , at miscible conditions. For chemical process the objective is to use a combination of phase behavior and reduction of interfacial tension (IFT), for example surfactants or alkaline agents which are injected to displace oil. For mobility-control process the objective is to maintain favorable mobility ratios to improve the displacement efficiency, for example polymers for thickening water. For thermal process the objective is to lower viscosity of the oil by injection of thermal energy or in-situ generation of so oil could flow easier towards the production wells, for example steam injection or in-situ combustion.

Recently, there is an alternative and promising EOR technique called smart water that has been proven in the laboratory and field scale. Smart Water is made by the adjustment and optimization of the ion compositions of the injected fluid so that the change in the initial COBR-system equilibrium will modify the initial wetting condition.

By using this technique, the oil is easier to be displaced from the porous network by increasing the microscopic efficiency. This technique will use the injection of water with significantly lower salinity than the natural salinity of formation water. Smart water injection will recover extra oil after performing a secondary water flood with formation water, so that this technique can be characterized as a tertiary oil recovery method. Detail explanation about Smart Water EOR will be discussed in Chapter 3.

## 2.3 Displacement forces

In the reservoir, there are three types of forces that determine the flow of oil and water in the reservoir, which are capillary forces, viscous forces and gravitational forces. These different forces will be briefly outlined in the following sections.

### 2.3.1 Capillary forces

Capillary forces consist of the interplay of surface and interfacial tensions between fluids and rock, pore size and geometry and the wetting characteristics of the rock-fluid system<sup>14</sup>. Capillary pressure may be defined as the pressure difference across a curved interface between two immiscible fluids, or between the non-wetting phase and the wetting phase. The capillary pressure can be calculated from the following equation.<sup>13</sup>

$$P_c = P_o - P_w = \frac{2\sigma_{ow} \cdot \cos \theta}{r} \quad (4)$$

Where:

- $P_c$  : Capillary pressure
- $P_o$  : Oil-Phase pressure at a point just above the oil-water interface
- $P_w$  : Water-phase pressure just below the interface
- $r$  : Radius of cylindrical pore channel
- $\sigma_{ow}$  : Interfacial tension between oil and water
- $\theta$  : Contact angle measured through the wetting phase (water)

Therefore capillary pressure is related to interfacial tension of fluid (IFT), relative wettability of the rocks (through contact angle,  $\theta$ ) and pore size ( $r$ ). Capillary pressure may be positive or negative. The sign expresses in which phase the pressure is lower, which will always be in the wetting phase. Indication that water is the wetting phase and oil is the non-wetting phase can be observed from the positive values of the capillary pressure.

In a fractured reservoir the capillary forces may contribute significantly to the displacement process during imbibition, or oppose it during a drainage process. Fractured reservoirs need strong capillary forces to increase the capillary pressure. The capillary pressure will result in an increase of spontaneous imbibition from the fractured channels into the matrix blocks. This condition will lead to the increasing of oil displacement from the low permeability zones.

For sandstone reservoirs, which are usually unfractured, favors lower capillary pressure causing less residual oil entrapment. Refer to equation 4 the capillary pressure can be reduced by lowering the interfacial tension of oil-water and/or changing the contact angle by inducing a wettability alteration.

### 2.3.2 Viscous forces

Viscous forces in porous medium are reflected by lateral differential pressures that force the fluid to move through pore network of reservoir. When fluid is forced through the reservoir or core, viscous forces are used to overcome the capillary barrier in the pores. The forces must be bigger than the capillary forces in order to make the fluid flow.

If the porous network is seen as a number of capillary tubes, the pressure drop across each capillary can be calculated by Hagen-Poiseuille<sup>13</sup> as presented in equation 5.

$$\Delta P = - \frac{8\mu L \bar{v}}{r^2 g_{cc}} \quad (5)$$

Where:

- $\Delta P$  : Pressure across the capillary tube
- $\mu$  : Viscosity of flowing fluid
- $L$  : Capillary tube length
- $\bar{v}$  : Average velocity in capillary tube
- $r$  : Capillary tube radius
- $g_c$  : Conversion factor

A dimensionless group of variables which represented the ratio of viscous to capillary forces is defined as capillary number ( $N_{ca}$ ) as presented in the equation 6.<sup>13</sup> The capillary number is an important parameter during EOR process. Higher capillary number means reduction of oil entrapment in the pore. From the equation 6, capillary number increases

by increasing the viscosity or flow rate of displacing fluid or by decreasing IFT between displacing and displaced fluids.

$$N_{ca} = \frac{F_v}{F_c} = \frac{v\mu_w}{\sigma_{ow}} \quad (6)$$

Where:

- $F_v$  : Viscous forces
- $F_c$  : Capillary forces
- $v$  : Interstitial pore velocity
- $\mu_w$  : Viscosity of water
- $\sigma_{ow}$  : Interfacial tension between oil and water

### 2.3.3 Gravitational Forces

The gravitational forces are caused by the density differences between two or more fluids. Gravitational forces will dominate of the flow, when there is large density difference between injected and displaced fluid, as well low interfacial tension between the fluids, in the thick reservoir. The buoyancy forces are always present in mixtures of immiscible fluids, and the lighter phase experiences a pressure pointing upwards, given by the equation 7.<sup>13</sup>

$$\Delta P_g = \Delta\rho \cdot g \cdot h \quad (7)$$

Where:

- $\Delta P_g$  : Pressure difference between oil and water due to gravity
- $\Delta\rho$  : Density difference between oil and water
- $g$  : Acceleration due to gravity
- $h$  : Height of the liquid column

In laboratory experiments with core samples, the gravitational effects are negligible, as the core diameter is only 3.8 cm

## 2.4 Wettability

Wettability is defined as the tendency of one fluid to spread on or adhere to a solid surface in the presence of another immiscible fluid<sup>15</sup>. When two immiscible phases are located together in a solid surface, one phase is usually more attached to the solid than the other one. The stronger attached phase is called the wetting phase. In the reservoir where oil and water exist together there will be oil wet and water wet systems. For oil wet case, oil phase wetting grain surfaces while water phase located in the pore bodies. For the water wet case, water phase wetting grain surfaces while oil phase located in the pore bodies. A reservoir may have mix wet condition when smaller pores are water wet and filled with water, whereas larger pores are oil wet and filled with oil. Figure 7 shows the oil-water position for respective wettability condition.

Reservoir rock wettability is an important factor when determining the success of waterflooding. It affects the location, flow and distribution of the fluids in the reservoir<sup>4</sup>. It also gives influence on capillary pressure and relative permeability for a two phase flow.

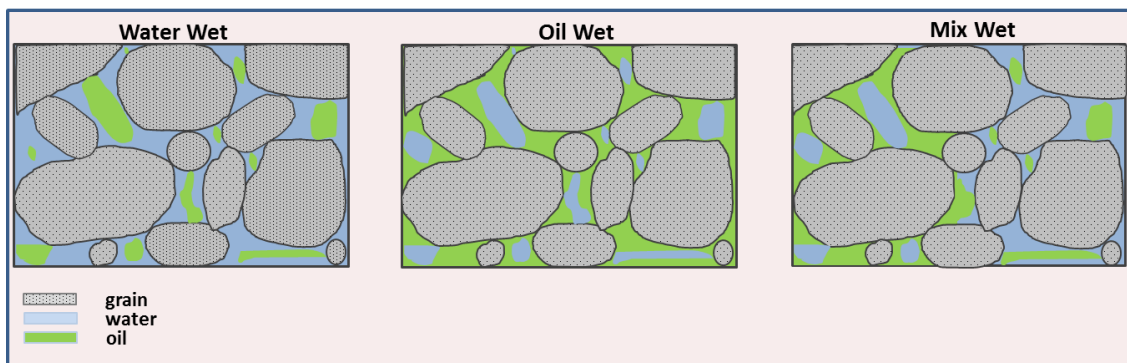


Figure 7. Fluid distribution in wetting condition

### 2.4.1 Wettability Measurement

Several methods have been developed for measuring the wettability of fluid/rock system both quantitatively and qualitatively.<sup>15</sup> The quantitative methods are direct measurement methods, where the wettability is measured on actual rock sample using reservoir fluid. The quantitative methods consist of contact angles, Amott test, and U.S. Bureau of Mines (USBM) wettability method. The qualitative methods includes, imbibition rates, microscopic examination, flotation, glass slide method, relative permeability curve, capillarimetric method, displacement capillary pressure, reservoir logs, nuclear magnetic resonance and dye adsorption. In this chapter, contact angle method and Amott method that related to this thesis, will be explained further.

Contact angle is defined as a tangent of oil-water surface in the triple point solid-water-oil, measured through water phase as illustrated in Figure 8. The contact angle is the best method to measure wettability when artificial cores and pure fluid are used.<sup>15</sup> However, it is not a suitable wettability measurement method when mineralogy varied in the porous medium.<sup>16</sup> Contact angle can be quantified from Young's equation as presented in the equation 8.<sup>13</sup>

$$\sigma_{ow} \cdot \cos \theta = \sigma_{os} - \sigma_{ws} \quad (8)$$

Where:

- $\sigma_{ow}$  : Interfacial tension between water and oil
- $\sigma_{os}$  : Interfacial tension between solid and oil
- $\sigma_{ws}$  : Interfacial tension between solid and water
- $\theta$  : Contact Angle

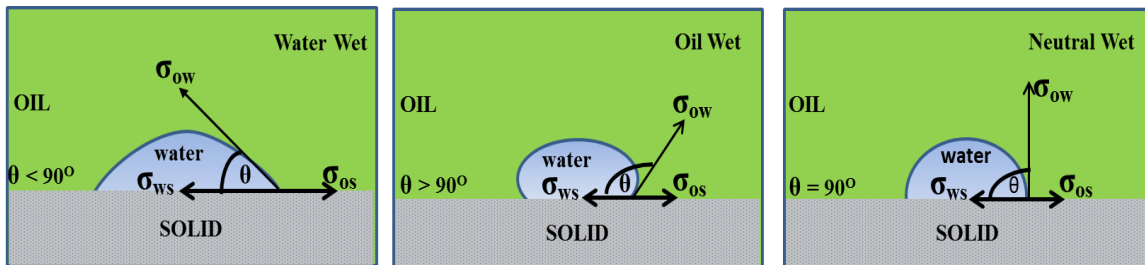
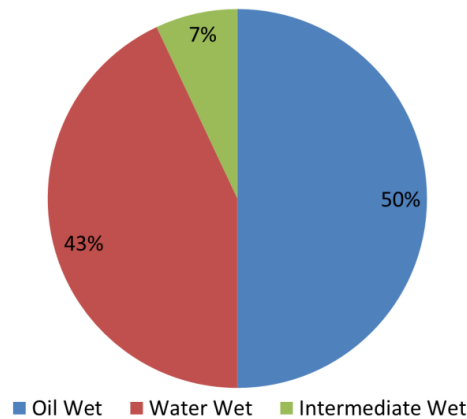


Figure 8. Contact angle wettability measurement illustration

The wettability of the rock can be classified based on the degrees of the contact angle. Table 2 shows the relationship between contact angle and wettability preference. Treiber et al.<sup>17</sup> reported wettability distribution of 32 sandstone reservoirs based on their contact angle, the result is presented in Figure 9.

Table 2. Contact angle and wettability preference<sup>6</sup>

Contact angle	Wettability Preference
0°-30°	Strongly water-wet
30°-90°	Preferentially water-wet
90°	Neutral wettability
90°-150°	Preferentially oil-wet
150°-180°	Strongly oil wet



**Figure 9. Initial wetting distribution over 32 sandstone reservoirs. Data is taken from Treiber et al.<sup>17</sup>**

### 2.4.2 Wettability Impact on Oil Recovery

Understanding reservoir wettability is crucial for optimizing oil recovery. The wetting preference influence many aspects of reservoir performance, particularly in waterflooding and enhanced oil recovery technique. Making the assumption that reservoir is water wet, when it is not, can lead to irreversible reservoir damage. Amott presented some earlier work on correlation between rock wettability and oil recovery by waterflooding<sup>17</sup>. This study indicates that low oil recovery or high residual oil saturation are obtained at either wettability extremes, whereas somewhat higher recoveries or low Sor are obtained in the weakly water wet to neutral wettability conditions as shown in the Figure 10a and Figure 10b.

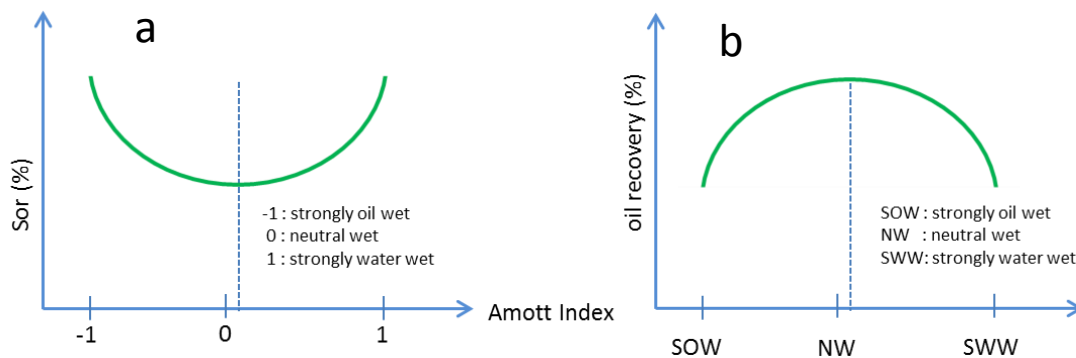


**Figure 10. Residual oil saturation vs Amott Harvey Wettability Index. Adapted from Skauge<sup>18</sup> (a) and Oil Recovery vs wetting conditions. Adapted from Strand<sup>16</sup> (b)**

### 3 SMART WATERFLOODING

From conventional point of view, the injected brine composition and ions were believed to have no effect on the recovery efficiency during waterflooding process.<sup>2</sup> So usually the nearest and cheapest water source, seawater or produced formation water, are used as injected water. Injection by fresh water is not a favorable choice due to the fact that it may lead swelling of some clays which creates serious reservoir problems and permeability reduction.

Recent researches conclude that smart or low salinity waterflooding can enhance the oil recovery by altering the initial wetting between crude oil, brine, and rocks. In this technique, brine with significantly lower salinity than the natural salinity of formation water will be used. Problems associated with conventional water flooding, such as scale formation, souring, and filtration at the ion levels can be mitigated with low salinity brine injection. On the other hand, it is affordable and environmental friendly EOR method.

#### 3.1 Low Salinity History

Reducing brine salinity to improve oil recovery is a relatively new theory. In fact, the first experiment testing this hypothesis was published as early as 1967. Bernard<sup>19</sup> found increased oil recovery when the sodium chloride content of the injection brine was lowered to 0.1%. Even though this is a field that goes back to the 1960s, but Tang<sup>10</sup>, Morrow<sup>10</sup>, Lager<sup>20</sup>, and Austad<sup>3</sup> have re-energized it in a remarkable way in the last couple decades. Oil companies such as BP<sup>20</sup>, Shell<sup>21</sup>, Total<sup>22</sup>, Saudi Aramco<sup>23</sup>, and Statoil<sup>24</sup> have also demonstrated a great concern in low salinity water flooding as an EOR method by investing in several research projects.

Among all the oil companies, BP has the greatest experience regarding to the low salinity waterflooding studies. Based on laboratory tests from different sandstone reservoirs, BP reported that the average increase in oil recovery factor was about 14%.<sup>20</sup> From the first trial from a single-well test, BP concluded a 25-50% reduction in residual oil saturation when waterflooding with low salinity brine during a log-inject-log field test in a sandstone reservoir.<sup>25</sup> In 2016, BP will start to apply for the first field scale implementation of low salinity waterflooding at Clair Ridge Field by expecting additional reserves around 42 million barrels oil. The additional lifting cost is only 3\$/barrel, much cheaper than the other technique about 20\$/barrel.<sup>26</sup> This lifting cost shows that low salinity waterflooding is still able to generate profit, eventhough at low oil price.

However, several experiments and field trials have yielded different findings. Zhang and Morrow<sup>27</sup> observed no increased oil recovery in secondary mode for a crude oil/Berea sandstone system, but a significant increase in tertiary mode for the same combination. In other case, Reinholdtsen et al.<sup>28</sup> also reported no increased oil production for Snorre field though the low salinity screening criteria already fulfilled before. Detailed explanation about the low salinity case in Snorre field will be explained further in chapter 3.5.

### 3.2 Condition For Low Salinity Effects

Austad<sup>3</sup>, Lager<sup>20</sup>, Tang and Morrow<sup>29</sup> summarized several desirable conditions of which low salinity may take effect as followed:

1. Porous Medium  
Significant clay fraction must be present. A type of clay may also play a role.
2. Oil  
Oil must contain polar components (acid/basic). No effect was observed in experiments with refined oil.
3. Formation Water  
Presence of formation water containing divalent cation ( $\text{Ca}^{2+}$  and  $\text{Mg}^{2+}$ ).
4. Injected Brine  
The salinity of injected brine is usually between 1,000-2,000 ppm, but effects have been observed up to 5,000 ppm.
5. Produced Water
  - For a non-buffered system, the pH of the produced water usually increases about 1-3 pH units, when injecting the low salinity brine.
  - In some cases, production of fines have been detected, but low salinity effects have also been observed without visible production of fines.
6. Permeability  
Both an increase and a decrease in differential pressure over the core has been observed by switching from high to low salinity fluid, which may indicate a change in permeability.
7. Temperature  
There is likely to be no temperature limitations to where low salinity effects can be observed. However, most of the reported studies have been performed at temperatures below 100°C.

### 3.3 Wettability Alteration

As described in the chapter 2.3, wettability in petroleum context is the tendency of reservoir rock to preferentially contact a particular fluid in a multiphase fluid system. This property is affected by the wetting condition of the rock as a result of interactions between crude oil, formation water and the rock itself. Wettability might change if there is a significant modification in one or more of those parameters. The content of minerals, ions, and hydrocarbon components are very important in determining wettability of the rock. In the real case, we can only change the properties of injected brine. It means if the produced formation water is re-injected in the reservoir, the wettability alteration in the reservoir never be observed. Therefore, understanding the behavior of each parameter in the equilibrium state is essential to artificially modify wetting condition in reservoir.

Wetting condition of reservoir can be altered by modification of the equilibrium state. Austad et al.<sup>3</sup> stated that injecting low saline water can alter the reservoir wettability to become more water-wet. It takes place due to in low saline environment some oil components will be desorbed from the rock surface. The increment of the water wetness degree will trigger an increase in capillary trapping of the oil droplets. Figure 11 illustrates the wettability alteration by switching from high salinity brine into low salinity brine; the low salinity brine can imbibe to the bypassed pores and mobilizes oil in the reservoir that is not swept by high salinity brine.

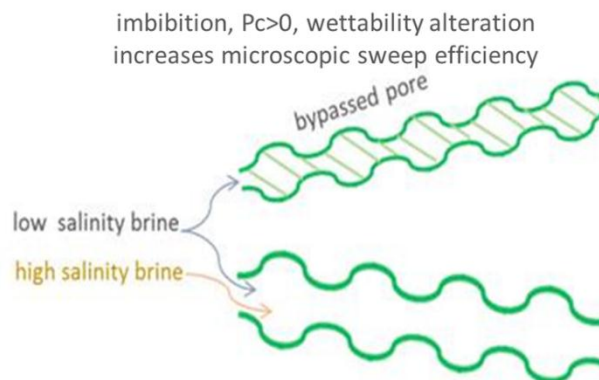


**Figure 11. Wettability alteration in low salinity waterflooding (adapted from Strand and Puntervold <sup>30</sup>)**

Strandnes<sup>31</sup> outlined some important parameters that have significant effect in wettability alteration as followed:

- Polar ionic hydrocarbon molecules that compose the oil
- Mineral composition of the rock
- Dissolved ions and salinity of the formation water
- Water solubility of polar oil components

- Pressure, temperature, and initial water saturation of the reservoir
- Capillary pressure

In this following sections, the most important wetting parameters will be briefly discussed to evaluate their impact on different wetting conditions observed for sandstone reservoirs.

## 1. Crude Oil

Several studies found that polar organic compounds such as acidic and basic organic material, dissolved in the crude oil may affect in altering wettability if they are adsorbed onto the surface of the rock. The acidic material present in the crude oil is mainly represented by carboxylic group, -COOH, which is mostly part of large molecules of the heavy end fraction of crude oil like the Resin and Asphaltene fraction. The basic material contains nitrogen as part of aromatic molecules,  $R_3N$ , with reactive pairs of electrons of the pyridine type. As they contain more polar compounds, this may result in generating electrical charged for both the oil and rock interfaces when presented with formation water.<sup>30</sup>

Buckley<sup>32</sup> described that there are several mechanisms of wetting properties alteration on a rock surface as followed:

- Polar interactions that predominate in the absence of a water film between oil and solid.
- Surface precipitation, depending mainly on crude oil solvent properties with respect to asphaltene.
- Acid/base interactions that control surface charge at oil/water and solid/water interfaces in the presence of water
- Ion binding or specific interactions between charged sites and higher valency ions.

Buckley also stated that the ability of the crude oil in altering the wetting properties can be identified by evaluating its following parameters: API gravity, acid number (AN) and base number (BN), or known as GAB parameters. For the  $AN=X$ , this means that X mg of KOH is needed to neutralize the acidic components present in the 1 gram of crude oil. For the  $BN=Y$ , Y mg KOH represents the equivalent amount of basic material present in 1 gram of oil.

The adsorption/desorption process of acidic and basic material mostly depends on its pH, ion composition of the brine and the type of clay mineral in the sandstone. Although both acidic and basic material can adsorb onto clay minerals, Austad<sup>3</sup> found from that similar effect appears on crude oil with high AN and low BN, and crude oil with high BN

and low AN when low salinity waterflooding took place. Therefore he concluded, during low saline flooding, it is likely to be no restriction on the type of polar components present in the oil.

## 2. Formation Water

The wetting state of an oil reservoir is greatly influenced by the pH of the formation water. The pH determines surface activity of active organic components against minerals especially clay. When salinity of the formation water is low, the availability of acidic gases such as CO<sub>2</sub> and H<sub>2</sub>S results in low pH of 5-6.5. Some minerals like Albite, can create alkaline environment in the reservoir when the formation water salinity is reasonably low.<sup>28</sup>

In general, the formation water salinity ranges from 10,000 to 25,000 ppm, which is influenced by the availability of common ions belong to alkali and alkali earth metal such as Na<sup>+</sup>, K<sup>+</sup>, Mg<sup>2+</sup>, Ca<sup>2+</sup>, Sr<sup>2+</sup>, and Ba<sup>2+</sup>. The most common anions is Cl<sup>-</sup>, and small amount of HCO<sub>3</sub><sup>-</sup> and SO<sub>4</sub><sup>2-</sup> which is relied on the relative concentration of the cations.

Some cation really affects the wettability of the reservoir if present in the formation water. This cation is ordered bellow with the relative replacing power is generally ordered as:



In which H<sup>+</sup> has the strongest affinity towards the clay surface. Optimal low salinity effects depend on a balanced initial adsorption of active cations, protons (H<sup>+</sup>) and organic materials on the clay surface.

## 3. Rock

Mineral composition and surface charge of the reservoir rock also have significant contribution in altering rock wettability. In sandstone reservoirs, clay and its cation exchange capacity play a major role for the wettability alteration. Some minerals like plagioclase<sup>22</sup> and anhydrite (CaSO<sub>4</sub>)<sup>30</sup> can give influence on the performance of low salinity waterflooding. Anhydrite solubility decreases as temperature increases, resulting dissolution of Ca<sup>2+</sup> in a low-salinity flooding which increases the concentration of Ca<sup>2+</sup> in the brine, which can affect the cation exchange process in the clay surface. Plagioclase is a group of poly silicates mineral that is often present in sandstone reservoirs. Albite with the chemical structure: NaAlSi<sub>3</sub>O<sub>8</sub> is often used as an example. It

can influence the initial pH of the formation water in the the reservoir. Field case and laboratory study of plagioclase and anhydrite effect on low salinity waterflooding will be explained in chapter 3.5.3.

#### **4. Temperature**

The reservoir temperature influences the reactivity of the ions and the solubility of different compounds. All the chemical reactions are temperature dependent. Small divalent cations like  $Mg^{2+}$  and  $Ca^{2+}$  are strongly hydrated in water at low temperature, and the reactivity is decreased. At high temperature the hydration energy is reduced and it makes the ion's reactivity increase. Therefore, chemical reactions involving  $Ca^{2+}$  and  $Mg^{2+}$  are often exothermic in nature, and the adsorption of  $Ca^{2+}$  onto clay increases as temperature increases.

Anions like  $CO_3^{2-}$  and  $SO_4^{2-}$  are solvated by hydrogen bonding to water molecules, and at high temperature,  $T > 100^\circ C$ , the hydrogen bonds break, and the reactivity of species increases. Therefore, the solubility of  $CaSO_4$  (s) and  $CaCO_3$ (s) decreases as the temperature increases.<sup>30</sup>

#### **5. Injected Brine**

The injected brine should have a significant lower salinity than the initial formation water. This is necessary to create desorption of polar oil compounds from the clay surface. The salinity of injected brine is usually between 1,000-2,000 ppm, but effects have been observed up to 5,000 ppm.<sup>3</sup> Seccombe<sup>33</sup> suggested that to get additional recovery from dilute brine displacement, the injected brine should have salinity below the salinity concentration threshold. Shortly, when the salinity of the injected water is reduced then the low salinity effect may take place and can be significantly increased.

### **3.4 Suggested Low Salinity EOR Mechanism**

#### **3.4.1 Migration of Fines**

In 1999, Tang and Morrow<sup>10</sup> conducted an experiment to explain the low salinity mechanism. In high salinity brine, clays tend to be undisturbed thus makes the oil-wet nature that results in poorer displacement efficiency. In contrast, during low salinity

flooding, they found that fine particles, of which mainly kaolinite clay, were released from the rock surface, which mainly is sandstone. They concluded that fines mobilization, as shown in the Figure 12, exposed the underlying rock surfaces which cause the system to be more water-wet. Moreover, the release of clay particles could divert the flow of water towards the unswept area thus better the sweep efficiency.

Tang<sup>35</sup> has shown that fine migration is likely to occur during the low salinity flooding. However, field experiences show that the increase in oil recovery could be achieved with no fine migration observed. Therefore, it could be concluded that migration of fines might be an effect of the flooding but might not be the direct cause of the increased recovery. Figure 12 shows the migration of fines mechanism.

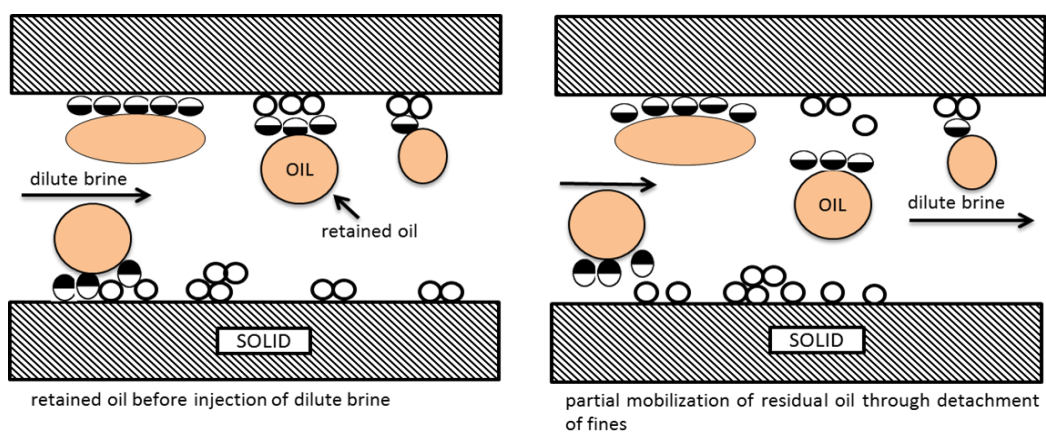


**Figure 12. Detachment of clay particles and mobilization of oil. Redrawn from Tang<sup>35</sup>**

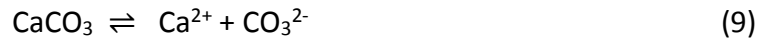
### 3.4.2 pH Increase

In 2005, McGuire<sup>36</sup> stated that low salinity water flooding could have similar effect to the type of alkaline flooding because of the pH increase that tends to occur during the process. Boussour<sup>37</sup> also added that the increase in pH level will allow the reaction of some of the oil compounds that result in generation of in-situ surfactants. Hence, by increasing the pH of the reservoir, the oil recovery could also be increased from the production of surfactant and interfacial tension reduction.

Lager<sup>33</sup> explained the occurrence of the event as an effect of these following chemical reactions:

- Increase in pH due to the cation exchange of  $H^+$  from the clay minerals that present in the liquid phase with the cations previously adsorbed. This type of reaction is relatively fast.

- Increase in pH due to the dissolution of carbonate minerals that causes an increase of ion OH<sup>-</sup> as presented in equation 9 and equation 10. This reaction is slower than the previous one, and depends on the amount of carbonate minerals of the rock.



### 3.4.3 Multi Ion Exchange

Multi ion exchange (MIE) between clay surfaces and injected low salinity brine has been suggested to be responsible for the EOR effect in the reservoir. Ionic equilibrium is being disturbed during the low salinity injection which caused the exchange to occur. Multi ion exchange (MIE) discuss about natural exchange between ions contained in the fluid and rock minerals, such as clay and carbonate, in the matrix. Experiment report of a low salinity waterflood on cores sampled from reservoir in the Northern Slope of Alaska shows that there was an indication on Mg<sup>2+</sup> adsorption onto the rock matrix during the injection of the brine. There were eight mechanism of organic matter adsorption onto clay mineral, as shown in the Table 3, proposed by Lager.<sup>38</sup> He stated that four of them were highly dependent on cation exchange occurred during a low salinity injection. Those are cation exchange; ligand bonding cation bridging and water bridging are illustrated in the Figure 13.

**Table 3. Mechanisms of organic matter adsorption onto clay mineral**

Mechanism	Organic functional group involved
Cation exchange	Amino, ring NH, heterocyclic N (aromatic ring)
Protonation	Amino, heterocyclic N, carbonyl, carboxylate
Anion exchange	Carboxylate
Water bridging	Amino, carboxylate, carbonyl, alcoholic OH
Cation bridging	Carboxylate, amines, carbonyl, alcoholic OH
Ligand exchange	Carboxylate
Hydrogen bonding	Amino, carbonyl, carboxyl, phenolic OH
Van der Waals interaction	Uncharged organic units

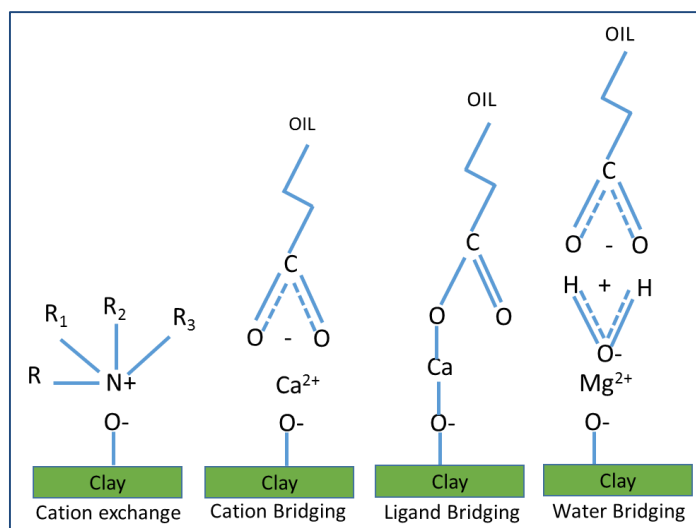


**Figure 13. MIE mechanism illustration. Redrawn from Lager et al.<sup>38</sup>**

The assumption of the process was that low salinity effect was related to the water wetness increase of clay minerals.  $Mg^{2+}$  and  $Ca^{2+}$  had an important role in the interaction between clay minerals and surface active components in the oil.  $Mg^{2+}$  and  $Ca^{2+}$  were likely to be a bridge between the negative charge of the clay surface and the positive carboxylic material. During the exchange, organic polar compounds and organo-metallic complexes will be removed from the clay surface and will be replaced by uncomplex cations. This will increase the water-wetness of the reservoir thus resulting in a recovery improvement.

### 3.4.4 Double Layer Effect

As explained before, cations will act like bridges between the negative oil components and clay surface. In 2009, Ligthelm<sup>39</sup> concluded that desorption of oil components from the clay surface can occur as a result of salinity reduction during the process which causes expansion of the electrical double layer between clay and oil interfaces. This desorption will increase the water wetness of the reservoir and increase the oil recovery.

### 3.4.5 Salting-in Effect

In 2009, Rezadoust et al.<sup>40</sup> have proposed terms that define changes in the solubility of polar organic components in the aqueous phase. These are then being identified as salting-in and salting-out effects. Salting-out effect is defined as the decrease in the solubility of organic material in water by adding salt to the solution, and vice versa.

These terms have been commonly found in many chemical literatures, and many experiments have also been conducted to observe both of these effects. Figure 14 below shows how ionic composition and water salinity affect the solubility of polar organic components.

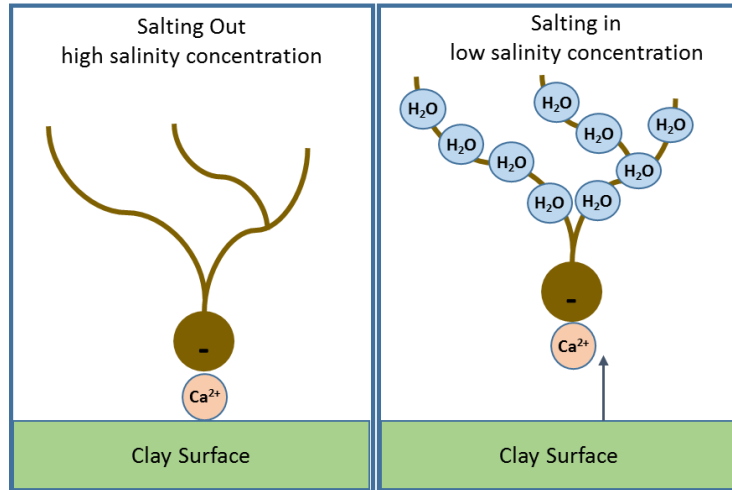


**Figure 14. Salting out and salting in mechanism illustration<sup>41</sup>**

Salting-in mechanism suggested that solubility of oil components in the reservoir water will increase as a result of low salinity injection that disrupts the equilibrium state between oil, water, and reservoir rock. This mechanism also increases the water wetness of the clay and boosts oil recovery. Later, experiment showed increased adsorption of polar oil components in low salinity than high salinity. This mechanism was therefore discarded.<sup>3</sup>

### 3.4.6 Desorption by pH Increase

Recently, Austad et al.<sup>3</sup> proposed another mechanism of low salinity waterflooding where desorption of initially adsorbed cations from the clay surface is the key process in the pH increase of the water. Low salinity brine will disturb initial equilibrium between COBR systems in the reservoir. Due to the lack of calcium amount in the injected brine, there will be ion exchange process between adsorbed cations in the clay surface and proton ( $H^+$ ) in the injected water. This process will increase the pH of water in the reservoir. This increase in pH will cause desorption of organic material from the clay surface. A basic principle to understand wettability alteration is the more amounts of organic materials adsorbed onto the clay surface the more oil-wet the reservoir will be. Thus, as the pH at the water-clay interface increases and resulting in the release of organic compounds from the clay surface, the wetting condition will then be altered to be more water wet. Therefore, it will be easier to displace the oil and increase the

recovery. Figure 15 illustrates the suggested mechanism process both for acidic and basic organic material.

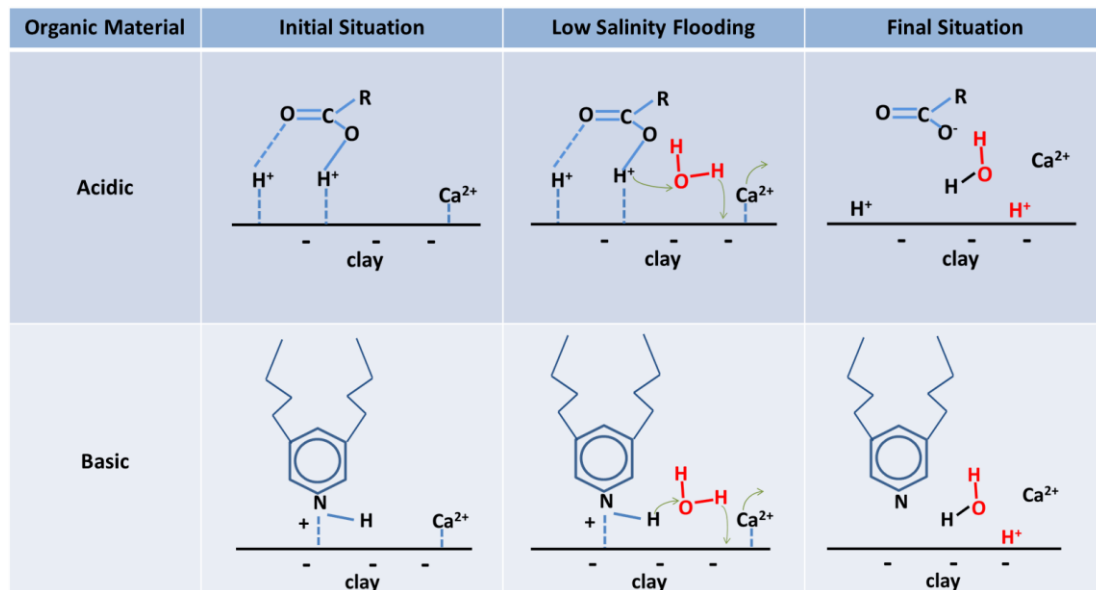
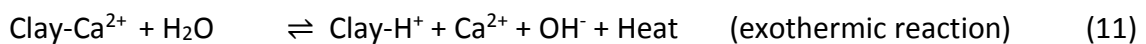


**Figure 15. Proposed mechanism for acidic and basic organic material desorption from clay surface during low salinity flooding, Redrawn from Austad et al.<sup>3</sup>**

This mechanism also can be stated in the chemistry reaction as shown in the following equation 11, 12, and 13.



This mechanism was studied further by Aksulu et al.<sup>42</sup> by investigating the adsorption of quinoline (basic organic material) onto illite at different numbers of pH for low salinity brine, LS (1,000 ppm) and high salinity brine, HS (25,000 ppm) as shown in Figure 16. It can be seen clearly that static adsorption of base onto illite was strongly dependent to the pH number and low salinity brine has higher adsorption compared to high salinity brine. Increase in pH number which is promoted by desorption of cations, is required to release oil components from the rock surface. As stated before, changes in pH number can be very sensitive to the adsorption of organic material onto the clay surface. Austad<sup>3</sup> observed that desorption of both acidic and basic crude oil materials took place as the pH number increases from around 5-6 to about 8-9. This shows that pH increase will reduce adsorption of oil components from clay surface.

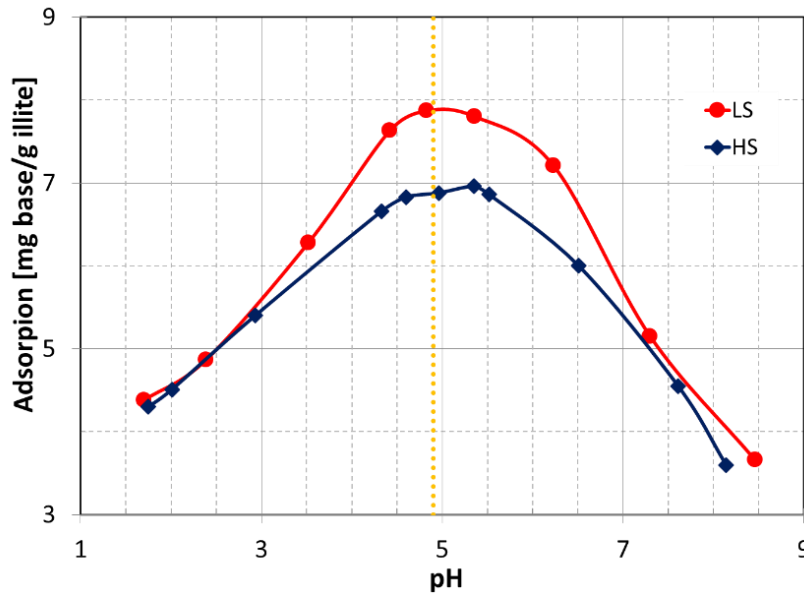


Figure 16. Adsorption of quinoline versus pH at ambient temperature in low salinity brine, LS (1,000 ppm), and in high salinity brine, HS (25,000 ppm). The dashed line represents the pKa value of quinoline (4.9). Redrawn from Aksulu et al.<sup>42</sup>

### 3.5 Laboratory and Field Case Study

#### 3.5.1 Relative Permeability

Fjelde et al.<sup>43</sup> investigated the effect of low salinity waterflooding on the relative permeability based on production history and pressure drop across the core. It was observed that the oil relative permeability increased after switching from formation water to a low salinity brine. It gave indication of wettability alteration in the core to be in more water-wet state. From their experiments, they also observed that there was no permeability reduction during low salinity waterflooding.

#### 3.5.2 Outcrop versus Reservoir Cores

In experimental study, outcrop cores and reservoir cores can be used to investigate the low salinity waterflooding performance. Both of them have different reservoir properties and mineralogy. Outcrop cores are usually used due to the limitation of reservoir cores storage.

Winoto et al.<sup>44</sup> has performed low salinity brine injection in outcrop cores and reservoir cores and evaluate the reduction of residual oil saturation. The overall result as presented in Figure 17 shows that the reservoir cores gave significant higher recovery or reduction of residual saturation compared to the outcrop cores. On the other hand, for field implementation projects, experiment with reservoir cores will give more reliable result because parameters such rock chemistry, rock properties, and initial wetting will be the same with the reservoir condition.

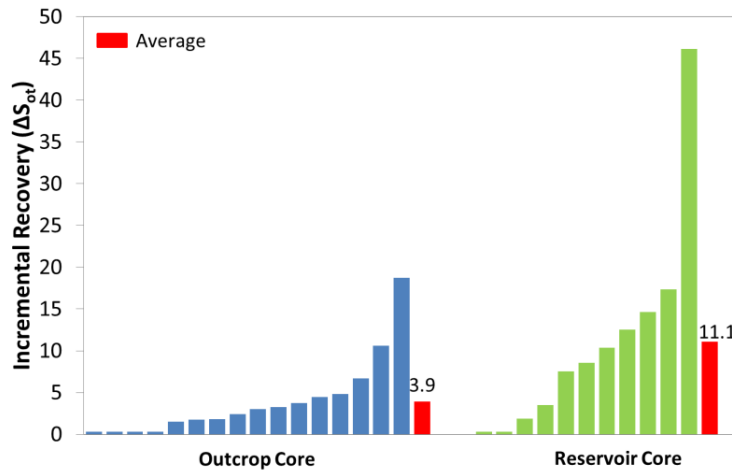


Figure 17. Incremental oil recovery from outcrop cores and reservoir cores. Redrawn from Winoto et al.<sup>44</sup>

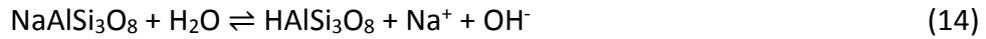
### 3.5.3 Mineralogy

- Plagioclase

Laboratory study from Snorre cores indicated a very low EOR effect of 2% of OOIP, even though the preliminary requirements for low salinity waterflooding have been fulfilled. There was no significant additional oil production after switching from Sea water (34,020 ppm) to the low salinity water (440 ppm). The interesting observation was the pH from the produced water was too high, around 10.<sup>45</sup>

Reinhorltsen et al.<sup>28</sup> tried to study further of Snorre cores. During the aging, the oil was saturated by CO<sub>2</sub>, it was expected to create pH below 7, but the result still gave the pH about 10. Further inspection of the core mineralogy showed that the Snorre cores contain significant amount of plagioclase, up to 35%. Plagioclase minerals have a buffering effect at moderate salinity of formation brine and will give an alkaline solution

according to the following reaction with the plagioclase is represented by Albite ( $\text{NaAlSi}_3\text{O}_8$ ) as the most common of plagioclase mineral that exist in the reservoir:



The initial  $\text{pH} > 7$  will make the rock too water wet for observing large LS EOR effect, which will decrease adsorption of basic and acidic components from the crude oil onto the clay minerals.<sup>22</sup>

In another case, Quan et al.<sup>46</sup> observed that reservoir core material containing high amounts of both plagioclase and clay, in the range of 20 and 25 Wt %, responded LS EOR effect with an increase in oil recovery of about 15% of OOIP. The salinity of the FW was about 63,000 mg/L, and the initial pH was 6.5. As the HS water was exchanged with the LS water the pH increased rapidly to 9.5, i.e. a factor of 3 pH units. Obviously, in this case also the plagioclase contributed to the increase in pH in the LS EOR process. Also the salinity of the FW was high enough to keep the initial pH well below 7. Thus, the learning from this work is that plagioclase minerals, if present in the reservoir rock, can have both positive and negative effects on the LS EOR process depending on the salinity of the formation water.<sup>22</sup>

- **Anhydrite**

It has also been noticed that high temperature and high salinity reservoirs containing anhydrite,  $\text{CaSO}_4$  (s), will suppress the desorption of  $\text{Ca}^{2+}$  from the clay surface as the HS water is exchanged with the LS water due to dissolution of anhydrite, i.e. the common ion effect.<sup>30,42</sup> Also in this case, equation 11 is moved to the left, and the increase in pH is smaller. It makes the relative replacing power of calcium stay high which prevents  $\text{Ca}^{2+}$  displacement by  $\text{H}^+$ , which finally will reduce the possibility desorption of polar organic compounds in the clay surface.

## 4 EXPERIMENTAL WORK

Laboratory experiment is a crucial element in the EOR project. It is conducted to assess the performance of the selected EOR method from the preliminary screening stage. Regarding smart water project, laboratory studies can provide the estimation of oil recovery as a function of the injected volume, information about the problems that may occur during the flooding process (scaling, swelling of clay, etc), and other waterflooding parameters. Finally it can suggest the optimal chemical composition to make the smartest injected water. This section describes experimental work research methodology in detail, and also outlines additional experiment using chemical analysis during flooding procedures and after.

### 4.1 Experimental Material

#### 4.1.1 Core

The experiment utilizes two reservoir sandstone cores, core-3 and core-5 from a field positioned offshore Norway in the southern part of the North Sea. Unfortunately, there is no X-Ray Diffraction (XRD) analysis of the core samples. The cores contain clay based on information from the company. Figure 18 shows picture of core-5. Table 4 lists important core data during the preparation of the core sample.

#### 4.1.2 Crude Oil

The company has provided the crude oil which had enough active organic material to stimulate organic adsorption onto the clay surface during core flooding and aging. Table 5 shows the oil properties. Base Number (BN) value is not provided due to technical failures of the BN instrument.



Figure 18. Core-5 captured from different angle

**Table 4. Physical core data**

Core	3	5
Length [cm]	7.03	7.25
Diameter [cm]	3.83	3.83
Bulk Volume [cm <sup>3</sup> ]	80.99	83.53
Pore Volume [cm <sup>3</sup> ]	11.35	11.64
Porosity [%]	14.0	13.9
Permeability [mD]	9	8.3

**Table 5. Oil properties**

AN (mg KOH/g)	Density (g/cm <sup>3</sup> )	Viscosity (cp)
0.16	0.835	7

### 4.1.3 Brine

These experiments used three different types of brines; they were formation water (FW), modified sea water (mSW) and modified low salinity water (LSm). The formation water was provided by company. The modified sea water was made from real sea water but depleted in SO<sub>4</sub><sup>2-</sup> to prevent scaling problems due to the formation water contain barium (Ba<sup>2+</sup>) and strontium (Sr<sup>2+</sup>). The modified low salinity water was made by diluting modified sea water twenty times. Table 6 lists ion composition and properties of the brine.

**Table 6. Chemical composition of brines**

Brine Ions(mM)	FW	SWm	LSm (d <sub>20</sub> SWm)
Na <sup>+</sup>	929.8	477.19	23.86
K <sup>+</sup>	17.8	8.12	0.409
Li <sup>+</sup>	0.0	0.0	0.0
Mg <sup>2+</sup>	7.0	13.5	0.679
Ca <sup>2+</sup>	44.2	8.24	0.412
Ba <sup>2+</sup>	5.2	0.0	0.0
Sr <sup>2+</sup>	3.0	0.0	0.0
HCO <sub>3</sub> <sup>-</sup>	7.7	0.333	0.017
Cl <sup>-</sup>	1058.8	527.86	26.39
SO <sub>4</sub> <sup>2-</sup>	0.0	0.4155	0.021
TDS, mg/L	63,000	30,725	1,536
Density (gr/cm <sup>3</sup> )	1.042	1.020	0.999
Salinity (ppm)	60,461	30,122	1,537

## 4.2 Experiment Steps

Figure 19 illustrates general steps for the experiment, which describes the overall process of the experiment on each core sample. The core restoration needs to be done on each core before injecting the core with water. Core restoration steps are shown in Figure 19 from brines and oil preparation until core aging. In this thesis, three viscous flooding experiments will be done on core-3 and core-5 as shown in Figure 20.

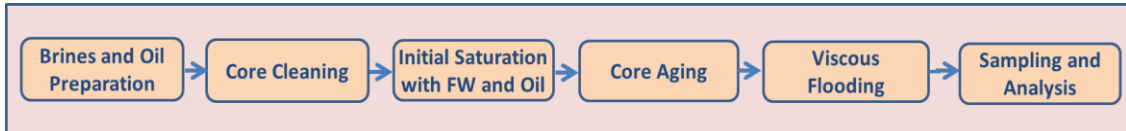


Figure 19. Schematic drawing of experiment steps

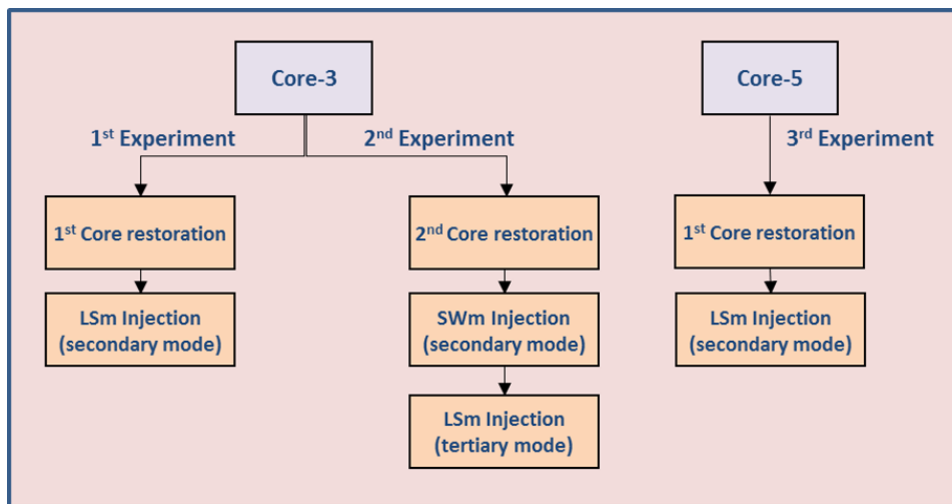


Figure 20. Viscous flooding experiment steps

### 4.2.1 Brines and Oil Preparation

#### 4.2.1.1 Brines Preparation

The LSm was made by diluting SWm. The dilution process was done by mixing SWm and deionized water (DI Water) until the concentration of LSm was 20 times lower than SWm. Once the brine was mixed, the next step was to filter the brine using a 0.22  $\mu\text{m}$  filter to remove any possible particles that could block the pore in the core. Figure 21 illustrates the filtration setup, composed of a Büchner flask, a vacuum pump and two-piece filtering funnel connected to the flask via a black elastomer, as an adapter for sealing. A filter and micro filter paper were placed in between two funnels and all of them were locked together to prevent any leakage. The vacuum pump was used to

syphon off the brine through the filter. Finally the filtered brine was collected in the flask and transferred to airtight flask.

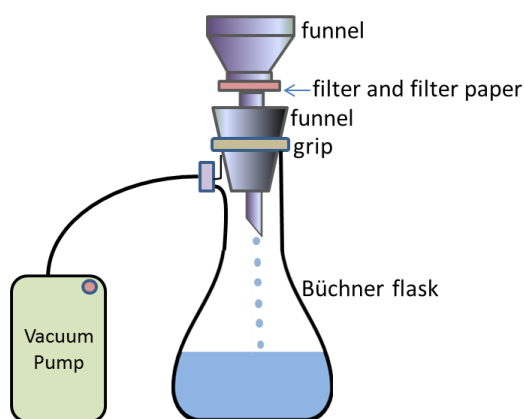


Figure 21. Water filtration setup illustration

#### 4.2.1.2 Oil Preparation

- **Oil Centrifuge and Filtration**

The crude oil needs to be purified from any impurities. First, centrifuge the oil to separate brines and heavy particles; however centrifuge system cannot separate small particles. Therefore those small particles can be removed by a filtration system as shown in the Figure 21. The setup is the same with water filtration unit.

- **Acid Number and Base Number Measurement**

The automatic titrator was used to determine the acid and base numbers of the oil. The automatic titrator used in this experiment was Mettler Toledo DL55 as shown in Figure 22. Different types of solvent were used for the measurement of AN and BN, however the procedure was the same. Detail procedures of AN and BN measurement are presented in the Appendix A.1.

- **Viscosity Measurement**

Universal dynamic spectrometer, Physical UDS 200 from Paar Physical (Figure 23), was used to determine liquid viscosity. Detailed procedure of viscosity measurement is presented in the Appendix A.2.



**Figure 22. Measurement of AN and BN by a titrator**



**Figure 23. Viscosity measurement by a spectrometer**

#### **4.2.2 Core Cleaning**

Before the core sample can be used in experiments, it should be cleaned from oil, formation brine, and contamination fluid during coring. This is performed in order to restore the initial wetting phase of the core sample which represents the actual subsurface condition. A proper solvent is usually used to extract all of the contaminants.

Conventionally, cores had been chemically cleaned by alternately administering vigorous solvents, for instance methanol and toluene. However, these chemicals had a tendency to dissolve polar components of the oil adsorbed onto the rock surface, finally it could alter the initial core's wettability. As maintaining the original rock properties was critical for the experiment, the cores were therefore cleaned using a mild cleaning process, as described in the following steps;

##### **1. Removing Oil Components by Kerosene**

As has been mentioned before all the cores were reservoir cores that still contain oil. Kerosene was flushed into the core to remove the initial crude oil. Different

from traditional cleaning which use methanol or toluene, flooding with kerosene is better at preserving the original wetting conditions of the core sample. The kerosene was injected, until the effluent color was acceptably clear, indicating that the core was ready for the next step of the cleaning process. Figure 24 shows the effluent of core cleaning process after flooded with kerosene.



**Figure 24. Effluents from kerosene cleaning**

## **2. Flushing with Heptane**

The cores were then flushed with heptane after completion of the kerosene injection. This would completely clean the core from kerosene, with minimal impact on the wetting conditions and polar components found on the rock surface. After clear effluent was observed, permeability measurement was done, which would be described in the next section.

## **3. 1000 ppm NaCl Flooding**

After the cleaning process with heptane, 1000 ppm NaCl was flooded into the core to remove formation water and any precipitated salts inside the cores. Pure DI water was not used in this stage because it could lead to clay swelling in the core. The effluent was collected and analyzed with Ion Chromatography (IC).

## **4. Core drying**

Finally the core was placed in a heating cabinet at 60°C to evaporate remaining liquids in the core. The core was dried in the heating cabinet until its weight gets constant after several measurements, marking that all the liquids had been evaporated.

### 4.2.3 Permeability Measurement

Permeability measurement was conveyed using heptane before the core drying process. The core was placed in a rubber sleeve inside a Hassler core holder. The core was flooded in one direction with heptane at different rate. The flooding rate was 0.05 ml/min, 0.1 ml/min, and 0.2 ml/min. 15 bars of confining pressure was applied to create one direction horizontal flow. The confining pressure was higher than the back pressure to ensure good sealing between the core and the rubber sleeve inside the core holder. The flooding was conducted at room temperature until a constant pressure drop across the core was achieved. The permeability of the core to heptane was then calculated from Darcy's law as shown in the equation 15. Since the experiments were performed using single phase, the heptane permeability was equal to the absolute permeability of the rock. Darcy's law is given by the following equation:

$$Q = \frac{kA\Delta P}{\mu_{heptane} L} \quad (15)$$

Where:

Q = Volumetric flow rate

k = Permeability

A = Cross section area of core

$\Delta P$  = Pressure difference across the core

$\mu_{heptane}$  = Viscosity of heptane

L = Length of core

### 4.2.4 Fluid Saturation

#### 1. Saturating Core with Diluted Formation Water

Firstly, the dry core was evacuated and placed on marbles inside a plastic container. Then it was put in a sealed setup. A vacuum pump was used to remove any air inside the setup. Then the diluted formation water was flowed through a valve, until water column was higher than the core height (the core is fully submerged). Figure 25 illustrates a setup schematic of the saturation apparatus. The dilution degree of formation water was calculated with the relation as seen in the equation 16;

$$n = \frac{1}{S_{iw}} \quad (16)$$

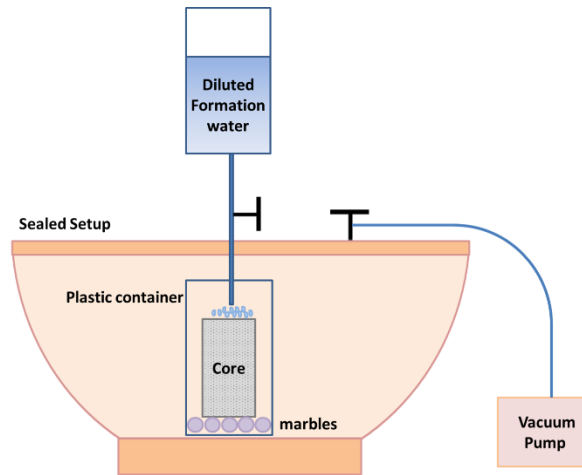


Figure 25. Schematic of equipment used for diluted formation water saturation to the core

## 2. Initial Water Saturation Establishment

The initial water saturation process refers to the method called desiccator technique developed by Springer et al.<sup>45</sup> After completion of diluted formation water saturation, the core was placed into a desiccator to evaporate the water as illustrated in the figure 24. Silica grains were put in the desiccator to increase the evaporation rate. During the evaporation process only distilled water that evaporated in the desiccator, and the salt stays in the core. It also explained the reason of fully saturate the core with diluted formation water instead of formation water in the beginning. The weight of the core was measured frequently until the core reached the target weight that corresponds to the desired initial water saturation (15%). Equation 17 shows the relation to calculate desired weight after evaporation process.

$$W_T = (W_s - W_d)S_{iw} + W_d \quad (17)$$

Where

$W_T$  = Target weight of the core at desired  $S_{iw}$  (gram)

$W_s$  = Weight of the core when saturated with water (gram)

$W_d$  = Dry weight of the core (gram)

$S_{iw}$  = Initial water saturation as a fraction of the pore volume

After the initial water saturation was achieved, the core was placed in a sealed container for few days to have equilibrium. This was done because during the evaporation process the water evaporated mainly from the outer part of the core. It would make the center part become more wet compared to the outer part of the core. Resting the core would

cause the water in the center part to settle outwards, creating uniform water distribution in the core.

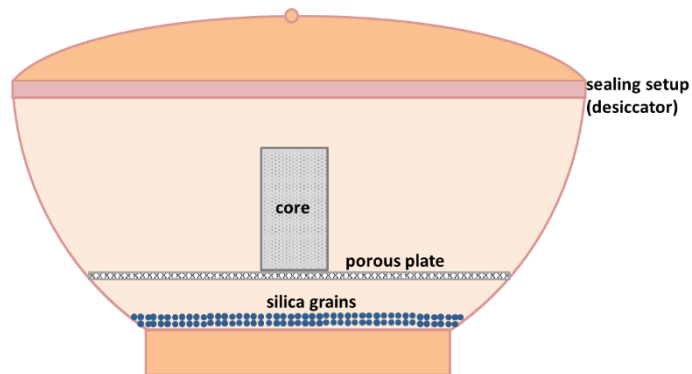


Figure 26. Desiccator illustration

### 3. Pore Volume and Porosity Calculation

The pore volume calculation was based on the weight difference between dry and wet core 100% saturated with diluted FW (6.7 times) with known density. Dry weight was measured after the core had been cleaned and dried. The wet weight was also measured after the core had been fully saturated with diluted formation water. Effective pore volume of the cores was calculated from equation 18. As well porosity of the core was calculated from equation 19.

$$PV = \frac{W_s - W_d}{\rho_{DFW}} \quad (18)$$

Where:

PV = Pore volume core [cm<sup>3</sup>]

W<sub>s</sub> = Weight of core 100 % saturated with diluted FW [gram]

W<sub>d</sub> = Weight of dry core [gram]

ρ<sub>DFW</sub> = Density of diluted FW [gram/cm<sup>3</sup>]

$$\Phi = \frac{PV}{V_b} \quad (19)$$

Where:

Φ = Porosity of core [%]

PV = Pore volume of core [cm<sup>3</sup>]

V<sub>b</sub> = Bulk volume of core [cm<sup>3</sup>]

## 4. Oil Saturation

The core with initial water saturation (15%) was mounted in the rubber sleeve and installed in the core holder. Confining pressure of 10 MPa was applied to the core holder. The air inside the flow lines were removed using a vacuum pump to prevent air bubbles coming to the core during oil saturation process. The experiment was done in the heating cabinet with temperature of 50°C. The pressure was set above the partial pressure of water to prevent evaporation of initial water in the core which could increase the formation water salinity. The oil was then injected with 2 pore volumes in each direction with the rate of 0.1 ml/min which consider as low rate to create a one dimension horizontal flow. Prior to the next step, the oven was turned off to cool down to the room temperature. It was done to prevent evaporation of volatile components from the oil in the core. Figure 27 illustrates a setup schematic of the saturation apparatus.

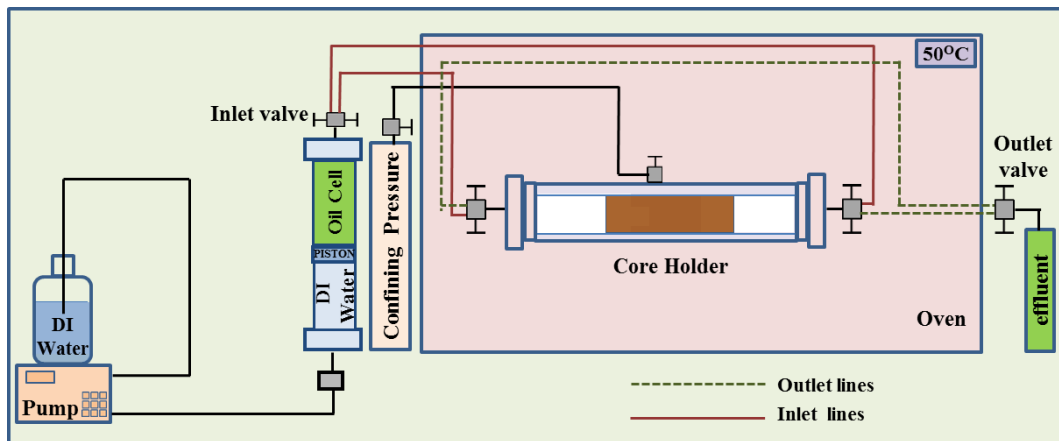


Figure 27. Oil saturation setup illustration

### 4.2.5 Aging of Core

After the core had been fully saturated with oil and formation water, the next step was aging of the core to create the initial wetting of the crude oil-brine-rock system at reservoir temperature. The saturated cores were wrapped in teflon tape and place on top of marbles in an aging cell that are already full of oil. The cells were then sealed and placed into heating cabinets at reservoir temperature 136°C for two weeks. 20 bar was applied to prevent boiling of initial water since the aging temperature above boiling point of water (100°C) and prevent evaporation of volatile component of the oil. During maturation, polar oil components could attach to the rock surface.

## 4.2.6 Oil Recovery Test

Oil recovery test was done by injecting water into the core to displace the oil. In this process viscous force was the main force related to the oil recovery. Gravitational force was neglected due to the diameter of the core that was less than 4 centimeters. The brine was injected through the core with the injection rate of 4 PV/D and created pressure drop across the rock, then the oil was produced followed by the brine in the effluent.

The schematic of the viscous flooding setup is shown in Figure 28. It can be seen that the setup consist of a pump, an oven, a Hassler core holder, piston cells, a measuring burette and a computer. The pump was connected to a computer program (Lab view) which determines the injection rate, minimum back pressure and maximum injection pressure. The program records inlet pressure, pressure drop across the core and temperature over the time. The core-holder was in principal simple device, which is linked to a pressure source, can employ pressure across the core, pushing fluids to move through the core laterally.

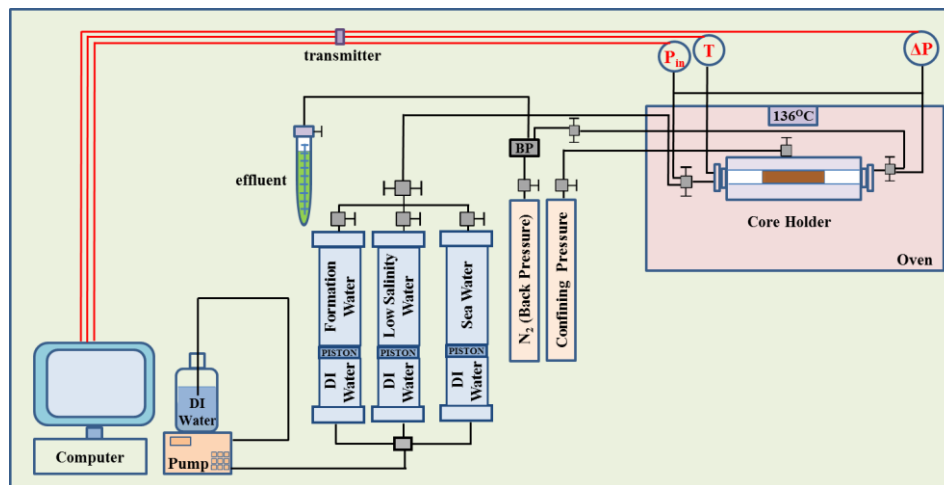


Figure 28. Oil recovery test setup illustration

A back-pressure valve (BPV) was used mainly to have almost constant pressure higher than atmospheric condition, avoid the water boiling of the formation water since the reservoir temperature above the water's boiling point, and prevent experiencing the volatile elements of the oil exposed from the core which could create three phase system. This was done due to the fact that during the oil recovery process at specific pressure drop value, volatile component changes to gas phase and made a three-phase system. Three phase system is more complex compared to a two-phase system, and experiencing gas bubbles in the core during the experiment would have been complicated when it comes to the integrity of the experimental results.

As mentioned before in the objective, this thesis was proposed to evaluate the waterflooding performance from different brines in the secondary and tertiary mode. First experiment was done using core-3 to investigate the performance of low salinity waterflooding in the secondary recovery mechanism mode. After the viscous flooding from the first experiment is finished, the core-3 was cleaned and followed the procedure to make the core ready for new flooding experiment.

Second experiment was done by reused core-3 to look into performance of low salinity brine in the tertiary recovery mechanism mode. During the flooding process, initially the core was injected by mSW brine until production plateau, and then followed by mLS brine. We would like to see whether there was production incremental after switching from medium salinity brine (Swm) to low salinity brine (LSm). It is also useful to compare the performance of low salinity waterflooding in the secondary recovery mode that has been done in the first experiment compare to the tertiary recovery mode. The last experiment was done using core-5 which was done in the secondary mode of low salinity waterflooding.

#### 4.2.7 Effluent Collection

During the oil recovery test, the effluent was collected in a graded burette. The volume of effluent could be monitored by the time from the scale in the graded burette. Results are presented as plots of oil recovery versus injected pore volumes of brine. The recovery factor was calculated from the following equation:

$$RF = \frac{V_p}{OOIP} \times 100 \% \quad (20)$$

Where:

- RF = Oil recovery factor (%)
- V<sub>p</sub> = Cumulative oil produced (ml)
- OOIP = Original oil in place (ml)

- **Effluent Analysis**

Several chemical properties such as pH, ion composition, and density are important parameters to have better understanding of the performance and mechanism behind waterflooding process with different types of brines.

- **pH Measurement**

During the flooding process, the effluent samples were collected in the seal samples chamber. The pH of the effluent samples was measured using a Mettler Toledo Seven Easy pH instrument (Figure 29). Prior to measuring the pH, the electrode was calibrated using buffer solution with pH 4, 7, and 10 to ensure the accuracy of the measurement. It is necessary to measure the pH immediately after the sample chambers are opened to avoid any chemical reaction between brine and CO<sub>2</sub> from air.

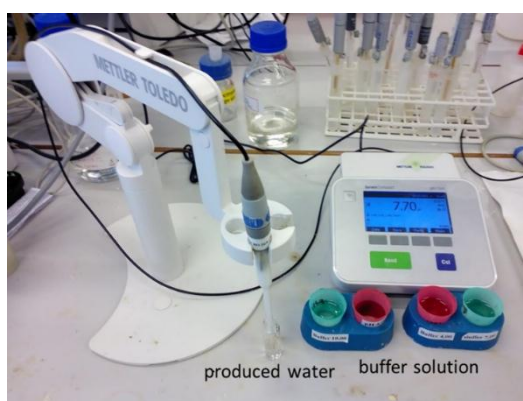


**Figure 29. Mettler Toledo Seven Easy pH instrument**

- **Ions Concentration Measurement**

Ion concentration from the effluent brine samples were measured using The Dionex ICS-300 Ion Chromatography (Figure 30b). To have optimum detection range for the IC, all the effluent samples were diluted 500 times and filtered through a 0.2 um filter. Dilution was handled by a syringe pump liquid handling setup by Gilson GX-271 Liquid Handler (Figure 30a). After the effluent were diluted and filtrated, the samples were poured into sealed sample bottles and placed in the IC Auto Sampler. Detail procedure of viscosity measurement is presented in the Appendix A.3.

The ions chromatography response of the samples were compared to the response of diluted standard water (FW, LSm, SWm, and normal SW) with known concentrations of the ions of interest. From the ion chromatography analysis, we could see the gradation of ion exchange during the flooding process by the time or by the pore volume of brine injected. Ion chromatography analysis is also a strong evidence to explain chemistry interaction for different brine during waterflooding process. All the ion were analyzed, but as Ca<sup>2+</sup>, Mg<sup>2+</sup>, and SO<sub>4</sub><sup>2-</sup> are the main active ions, this thesis presents the plot only for those three.



**Figure 30. Gilson GX-271 Liquid Handle (a) and Dionex ICS-3000 Ion Chromatography (b)**

- **Density Measurement**

Both density of brines and oil were measured by using Anton Paar DMA 4500 Density Meter shown in Figure 31. The measurements were performed at 20°C. Before the oil and brine samples were injected, the tube was cleaned with white spirit and acetone. It was critical that no gas bubbles penetrated during the injection of fluid for the accuracy. The measurements were done repeatedly for accuracy.

By measuring the produced water density, the gradation of mixture process between the initial formation water and different injection brines could be seen.



**Figure 31. Antoon Paar 4500 Density Meter**

## 5 RESULTS

Coreflood experiments were conducted to evaluate the smart water effect in two sandstone reservoir cores, core-3 and core-5. The experiments gave information about oil recoveries for both LSm and SWm in the secondary injection mode. At the end of SWm flooding, evaluation of low salinity EOR potential in tertiary mode by injecting LSm brine was conducted. In the experiment, formation water with relatively low salinity 60,461 ppm was used, which was good enough to have relatively mixed wet condition at high reservoir temperature. It was experimentally verified that at high temperature, relatively low formation water salinity could contribute to more adsorption of polar component from oil onto the clay surface.<sup>47</sup>

### 5.1 Oil Recovery Test on Core-3, 1<sup>st</sup> Restoration

Prior to the flooding experiment, core-3 was cleaned using kerosene and heptane. Then the core was restored and saturated with formation water and crude oil to stabilize initial condition, which were 15% and 85% of initial water ( $S_{wi}$ ) and oil saturation ( $S_{oi}$ ), respectively. The core was then aged in a heating chamber for two weeks under 10 bar pressure and 136°C reservoir temperature. Afterwards, the experiment was conducted by LSm injection for the secondary mode.

- **Oil Recovery Result**

Figure 32 presents the percentage of oil recovery to the original oil in place (OOIP) as a function of pore volume of brine injected. The figure 32 shows that recovery factor is dramatically increasing with constant slope until breakthrough of LSm at 0.46 PV which corresponds to 53.9% of OOIP.

Figure 32 also shows a reduction in the slope of oil recovery factor after 0.46 PV of LSm was injected. The slope changed because of the water breakthrough through the outlet of the core. After the water breakthrough, the injected water replaced both produced oil and produced water. Eventually it reached a point where there was no movable oil that could be displaced by LSm. The ultimate recovery factor was 63% of OOIP, it was reached after 3 PV of LSm was injected.

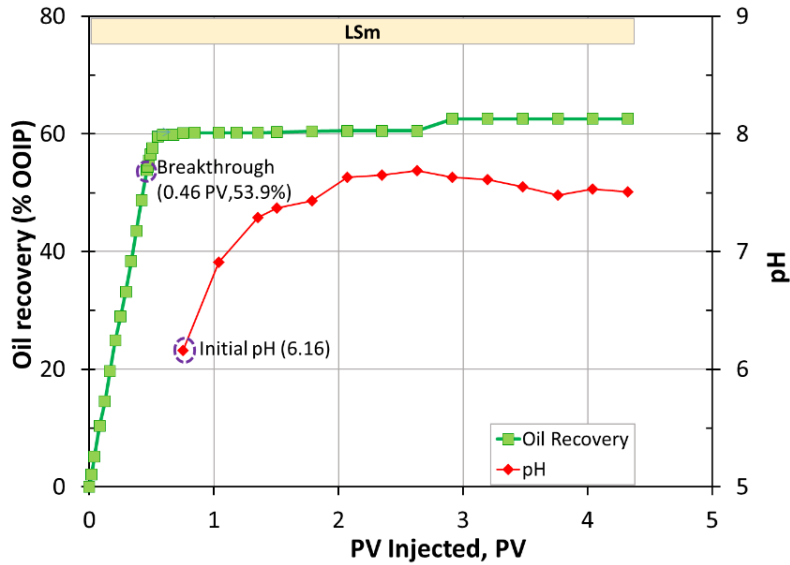


Figure 32. Oil recovery during the 1st restoration of core-3

- **Pressure Drop and Temperature**

Figure 33 shows pressure drop and temperature during the oil recovery test of core-3. In the beginning of the oil recovery test, the pressure drop was about 210 mbar and was fluctuating around 160-300 mbar. The fluctuating readings were recorded at the beginning of injection process which represented oil mobilization from the core during LSm injection. Then it declined to ~150 mbar at the end of LSm flooding process. It showed that the pressure drop across the core decreased as the oil saturation of the core decreased. Temperature was kept constant at 136°C during the entire experiment.

- **pH and Density**

Figure 34 shows the pH and density of the produced water (PW) during oil recovery of core-3. pH was measured at ambient temperature while density was measured at 20°C, as the temperature in the Antoon Paar 4500 Density Meter . Initial effluent pH came out at 6.16 pH unit and it increased up to 7.8 until and reached a plateau at 7.55 pH number. The initial pH value 6.16 showed acidic environment equilibrium in the restored core which indicated good condition for adsorption of polar oil component on the wetting surface of the rock. Meanwhile, produced water density profile drastically dropped from 1.025 gr/cc to around 0.999 gr/cc which was equal to the density of LSm after approximately 1.5 PV of LSm was injected. The density was then quite stable throughout the rest of the flooding process.

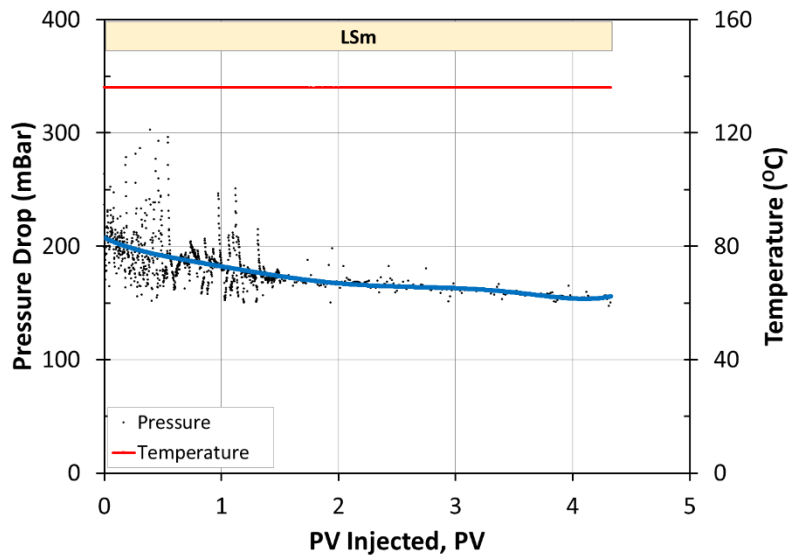


Figure 33. Pressure drop and temperature across the core during oil recovery test on core-3 (1<sup>st</sup> restoration)

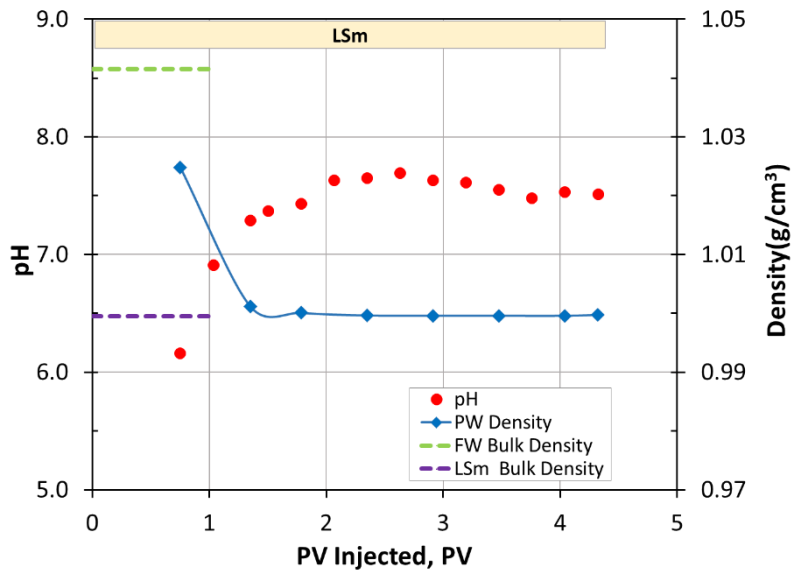


Figure 34. Produced water pH and density during oil recovery test on core-3 (1<sup>st</sup> restoration)

- **Ion Chromatography Analysis**

Figure 35 shows the concentration profile of calcium, magnesium, and sulfate from chemical analysis of the produced water in the 1<sup>st</sup> restoration of core-3. During the flooding process, all ions showed declining trend until it reached stabilization in its concentration profiles. Initial concentration from the produced water was 35 mM of Ca<sup>2+</sup>, 10 mM of Mg<sup>2+</sup>, and 4 mM of SO<sub>4</sub><sup>2-</sup>. As expected, the concentration of calcium

dropped significantly from 30 mM to 0.3 mM, as a transition from calcium rich formation water to the LSm which contained less calcium. The stabilized calcium concentration was 0.3 mM. It was close to the bulk calcium concentration of LSm, 0.4 mM. While magnesium concentration rapidly decreased from 10 mM to about 0.06 mM, the stabilized magnesium concentration was much lower than the bulk magnesium concentration of LSm, 0.6 mM.

Meanwhile the first produced water contained 4mM of sulfate, even though the displaced formation water did not contain any sulfate. This concentration declined as more LSm was injected until it reached stabilized sulfate concentration about 1 mM, which was much higher than bulk sulfate concentration in LSm, 0.021 mM.

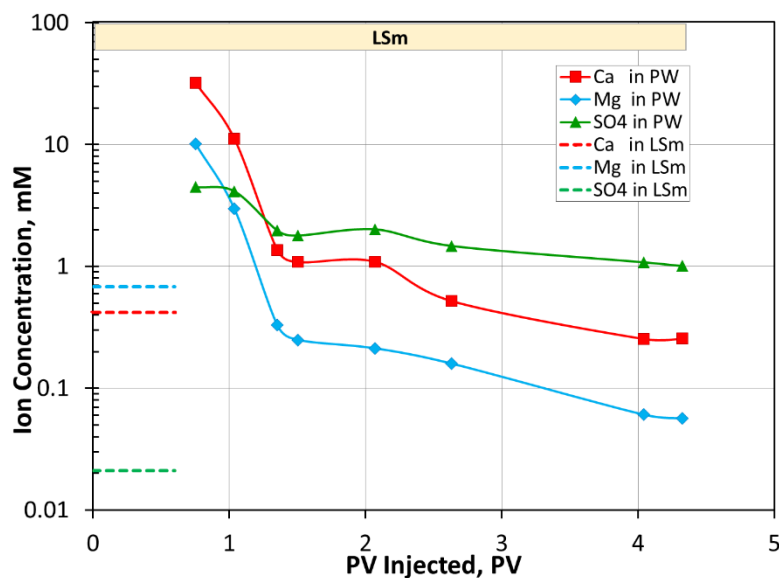


Figure 35. Ion chromatography analysis during oil recovery test on core-3 (1<sup>st</sup> restoration)

## 5.2 Oil Recovery Test on Core-3, 2<sup>nd</sup> Restoration

After the 1<sup>st</sup> restoration was completed, core-3 was then mildly cleaned. It was then restored and saturated with formation water and crude oil until it reached its initial saturation: 15% of  $S_{wi}$  and 85% of  $S_{oi}$ . Similar to the 1<sup>st</sup> restoration, the core was then aged in a heating chamber for two weeks under 10 bar pressure and 136°C reservoir temperature. Afterwards, the experiment was conducted by injecting SWm for the secondary injection mode and LSm for the tertiary mode. The Injection flow rate of both fluids were 4 PV/D. LSm flooding was then continued with a higher injection rate of 16 PV/D to see any possible end effect.

- **Oil Recovery Result**

In this experiment, SWm was injected during the secondary mode and followed by LSm injection in the tertiary mode. Figure 36 shows the percentage of oil recovery to the original oil in place (OOIP) as a function of volume injection brine into the core. The oil recovery factor during secondary mode (SWm injection) increased with constant slope until 0.42 PV of injected brine or corresponding to 46.5% recovery factor. After this point, the recovery factor gradually increased until it reached a plateau of 51 % of OOIP.

The process was then continued by LSm injection for the tertiary mode. This was conducted in order to examine how changes in salinity would affect the production performance by switching the injection process from medium salinity brine (30,122 ppm) to low salinity brine (1,538 ppm). The oil production gradually increased during LSm flooding. 9% increments was obtained before the production reached a plateau at 60% oil recovery, after 3 PV of LSm was injected. At the end of LSm flooding process, there was no extra oil production even though higher injection rate, 16 PV/D was applied.

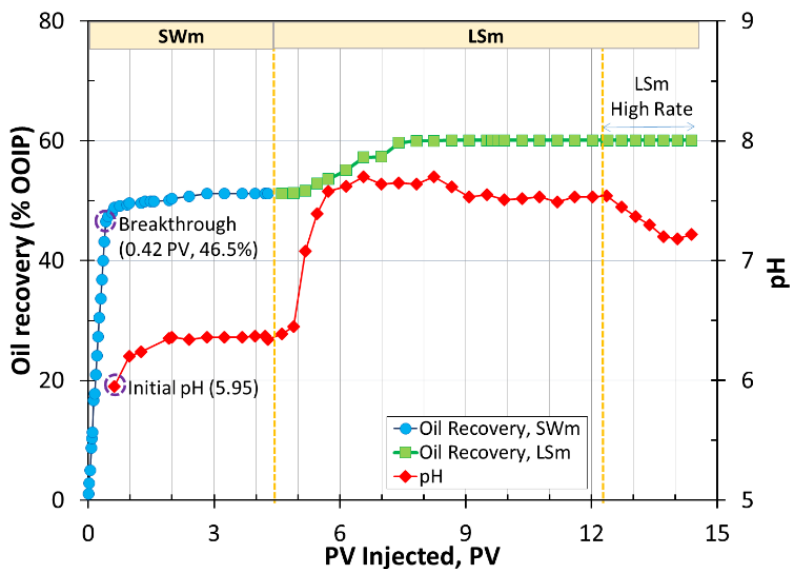


Figure 36. Oil recovery during the 2<sup>nd</sup> restoration of core-3

- **Pressure Drop and Temperature**

Figure 37 describes pressure drop and temperature during the oil recovery test of core-3 in the second restoration. Pressure drop profile during this 2<sup>nd</sup> experiment was similar to the 1<sup>st</sup> experiment. In the beginning of oil recovery the pressure drop was about 220

mbar and fluctuating around 150-240 mbar, then it declined to ~120 mbar at the end of SWm flooding and LSm flooding. The fluctuating readings were recorded at the beginning of injection process which represented oil mobilization from the core during the injection of SWm. It showed that pressure drop across the core decreased as the oil saturation of the core decreased. After switching from SWm to LSm, that the pressure drop across the core remained constant.

At the end of the flooding process, the injection rate was increased to 16 PV/D. Pressure drop increased significantly from 120 mbar to 420 mbar by increasing the rate four times. The increment of the pressure drop was proportional to the increment of injection rate. Temperature was kept constant at 136°C during the experiment.

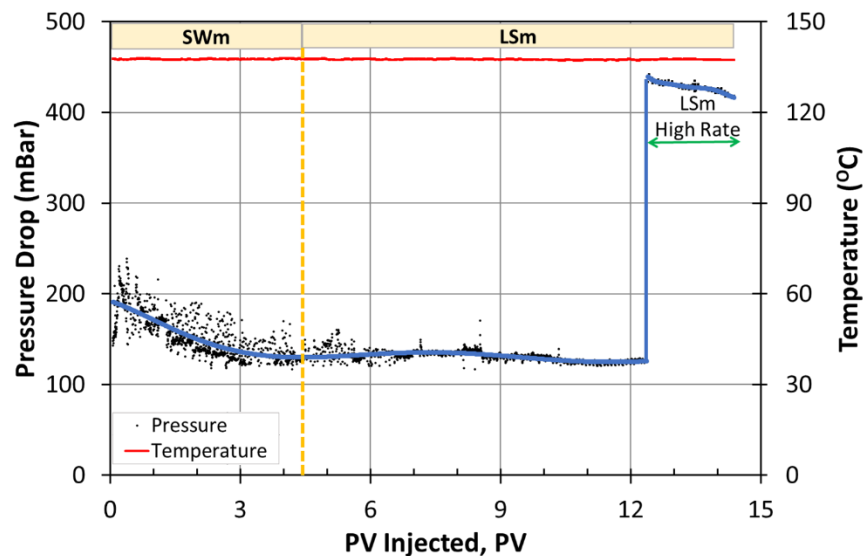


**Figure 37. Pressure drop and temperature across the core during oil recovery test on core-3 (2<sup>nd</sup> restoration)**

- **pH and Density**

Figure 38 shows the pH and density of the produced water during oil recovery of 2<sup>nd</sup> restoration of core. The pH was measured at ambient temperature while density was measured at 20°C, as the temperature in the Antoon Paar 4500 Density Meter. Initial effluent pH came out at 5.95 and gradually increased until reached plateau of 6.4 as more SWm was injected. The initial pH value, 5.95 showed acidic environment equilibrium in the restored core which indicated good condition for adsorption of polar oil component on the wetting surface of the rock.

After the injected brine was changed into LSm, the pH increased and reached a plateau of 7.5. The pH values slightly decreased to 7.2 after increasing the rate of LSm flooding to the high rate, 16 PV/D.

The produced water density decreased as more SWm was injected until reached its stabilized value. Initial effluent density was 1.035 gr/cc and decreased to 1.02 gr/cc (density of bulk SWm) during SWm flooding. Meanwhile, during the LSm flooding, the density of the PW was stable at 0.999 gr/cc which was equal to the bulk density of LSm.

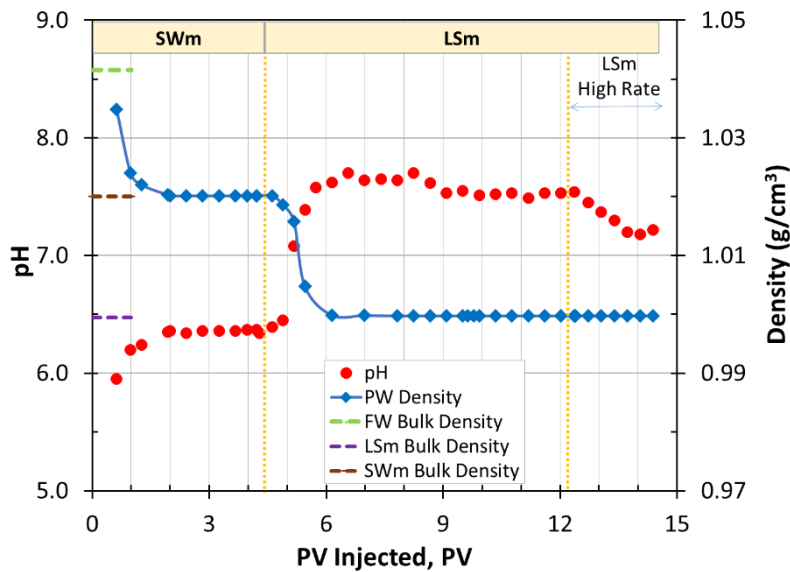


Figure 38. Produced water pH and density during oil recovery test on core-3 (2<sup>nd</sup> restoration)

- **Ion Chromatography Analysis**

Figure 39 shows the concentration of calcium, magnesium, and sulfate for chemical analysis of the produced water during second restoration of core-3. During the SWm injection, the ions concentration decreased as more SWm was injected until the concentration reached a plateau. As presented, initial concentration from the produced water was 50 mM of Ca<sup>2+</sup>, 18 mM of Mg<sup>2+</sup>, and 3 mM of SO<sub>4</sub><sup>2-</sup>. The stabilization of ions concentration during the SWm flooding was 12.5 mM of Mg<sup>2+</sup>, 9 mM of Ca<sup>2+</sup>, and 0.4 mM of SO<sub>4</sub><sup>2-</sup>. These stabilized values were quite close compared to the initial concentration of the ions in the SWm, which were 13.5 mM for magnesium and 8.3 mM for calcium. Meanwhile sulfate concentration decreased from 4 mM to 0.4 mM at the end of the flooding.

After the injected brine was switched from SWm to LSm with constant injection rate 4 PV/D, the ions concentration decreased further. The calcium and magnesium concentration reached a plateau as more LSm was injected, while sulfate concentration kept decreasing as more LSm was injected. Figure 39 shows magnesium and calcium concentration stabilizes at 0.4 mM and 0.05 mM, respectively, during LSm injection with constant injection rate 4PV/D. The stabilized calcium concentration was equal to the bulk concentration of the LSm brine, 0.4 mM. Meanwhile the stabilized magnesium concentration was 0.06 mM, much less than the bulk concentration of LSm, 0.67 mM. However, sulfate concentration slightly increased in the region 4.8-5.8 PV injected. Later on, the sulfate concentration decreased to 0.1 mM, which was higher than bulk sulfate concentration of LSm, 0.021 mM.

At the end of flooding process, the injection rate of LSm was increased to 16 PV/D. The calcium and magnesium concentration remained constant from the stabilized value during 4 PV/D injection rate. But sulfate concentration declined to 0.04 mM close to the bulk concentration of LSm 0.021 mM.

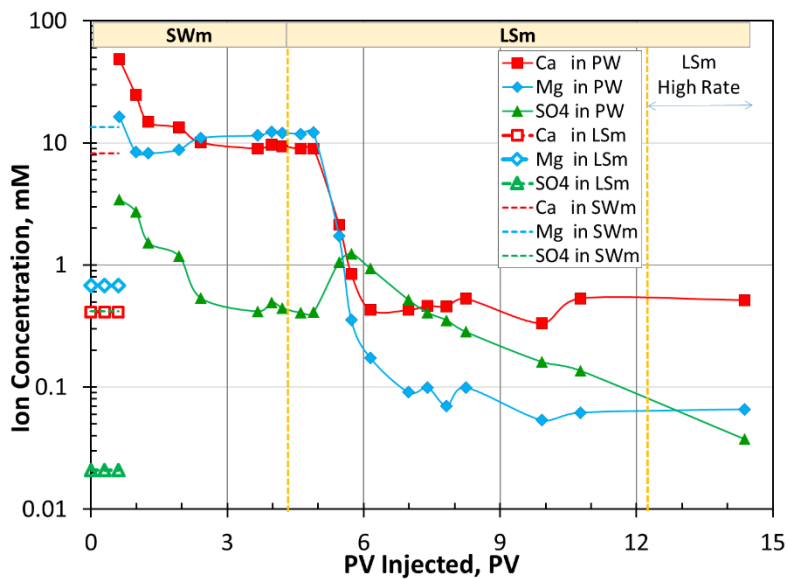


Figure 39. Ion chromatography analysis during oil recovery test on core-3 (2<sup>nd</sup> restoration)

### 5.3 Oil Recovery Test on Core-5, 1<sup>st</sup> Restoration

The third experiment was generally similar with the first one, LSm flooding in the secondary mode. The only difference was that the experiment utilized a new core (core-5) instead of reconditioning a used core like what was done in the 2<sup>nd</sup> experiment. Initial condition was set to be just like two previous experiments: 15% of  $S_{wi}$  and 85% of  $S_{oi}$ .

- **Oil Recovery Result**

Figure 40 presents the recovery profile during the flooding process. It can be noticed, that the recovery was drastically increased up to 52.6% of OOIP which corresponded to 0.45 PV of injected LS<sub>m</sub>. The recovery factor then gradually increased and it reached a plateau of 58% after injection of 1.2 PV LS<sub>m</sub>. The injection of LS<sub>m</sub> at rate 4 PV/day was continued until 4.5 PV of LS<sub>m</sub> was injected. Then the rate was increased to 16 PV/day to see any possible end effect. There was no additional oil recovery observed, during LS<sub>m</sub> high rate injection.

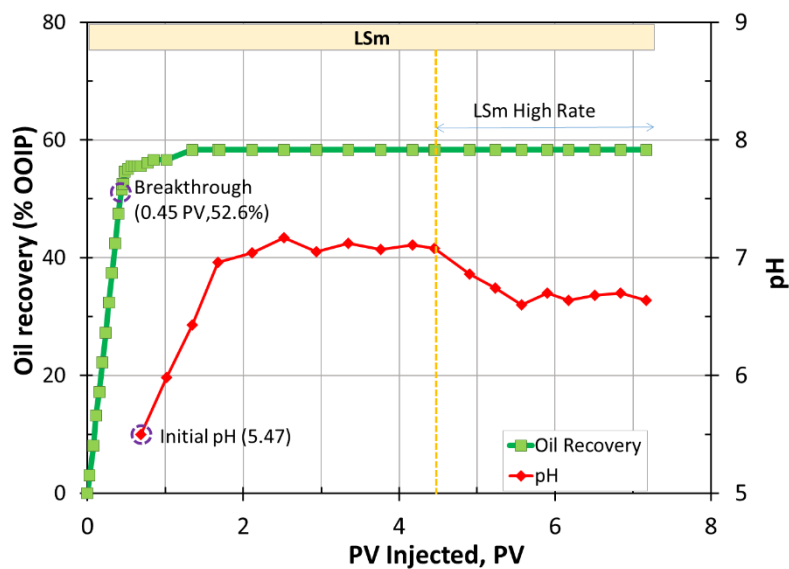


**Figure 40. Oil recovery during 1<sup>st</sup> restoration of core-5**

- **Pressure Drop and Temperature**

Figure 41 presents the pressure drop across the core during oil recovery of core-5 in the first restoration. Similar to previous experiments, it shows a high peak in the beginning of oil recovery process followed by pressure drop stabilization. The fluctuating readings around 150 mbar- 350 mbar were recorded at the beginning of injection process which represented oil mobilization from the core during the injection of LS<sub>m</sub>. Then the pressure drop across the core declined to ~170 mbar, with constant injection rate 4 PV/D. It showed that the pressure drop across the core decreased as the oil saturation of the core decreased.

In this experiment, we conducted the high injection flooding rate, 16 PV/D at the end of the flooding process, which made a higher pressure drop across the core. Pressure drop increased significantly from 170 mbar to 610 mbar by increasing the rate four times. The increment of the pressure drop was proportional to the increment of injection rate. The temperature was kept constant at 136°C during the experiment.

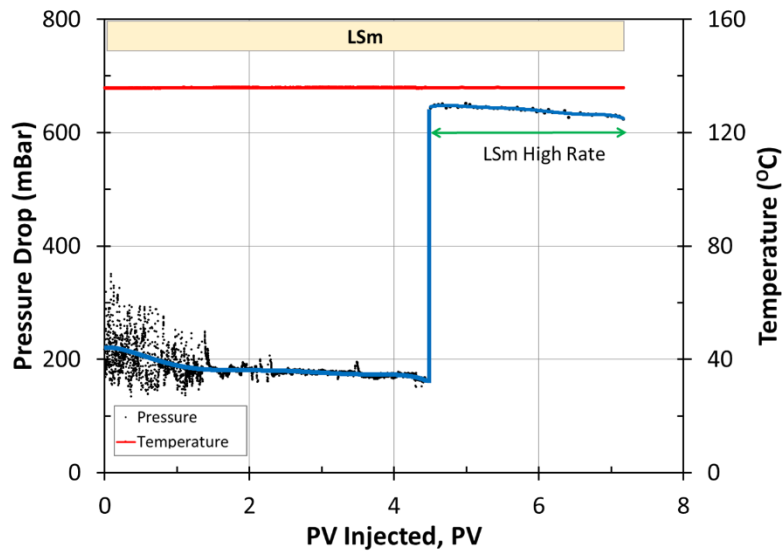


**Figure 41. Pressure drop and temperature across the core during oil recovery test on core-5 (1<sup>st</sup> restoration)**

- **pH and Density**

Figure 42 presents pH and density profiles of the produced water during oil recovery test of core-5. pH was measured at ambient temperature while density was measured at 20°C, as the temperature in the Anton Paar 4500 Density Meter. At the initial measurement, the produced water had the pH number of 5.5. The initial pH value of 5.5, showed acidic environment equilibrium in the restored core which indicates good condition for adsorption of polar oil component on the wetting surface of the rock.

As the flooding continues, alkalinity of the brine increased gradually and reached stability at the 7.2 pH number after injection of 2.1 PV of LSm brine at 4 PV/D injection rate. After switching the injection rate to 16 PV/D, the pH values slightly decreased to 6.6. Meanwhile, water density profile drastically dropped from 1.027 gr/cc to around 0.999 gr/cc (LSm bulk density) after about 2 PV of brine was injected. Then the density was stable throughout the rest of the flooding process.

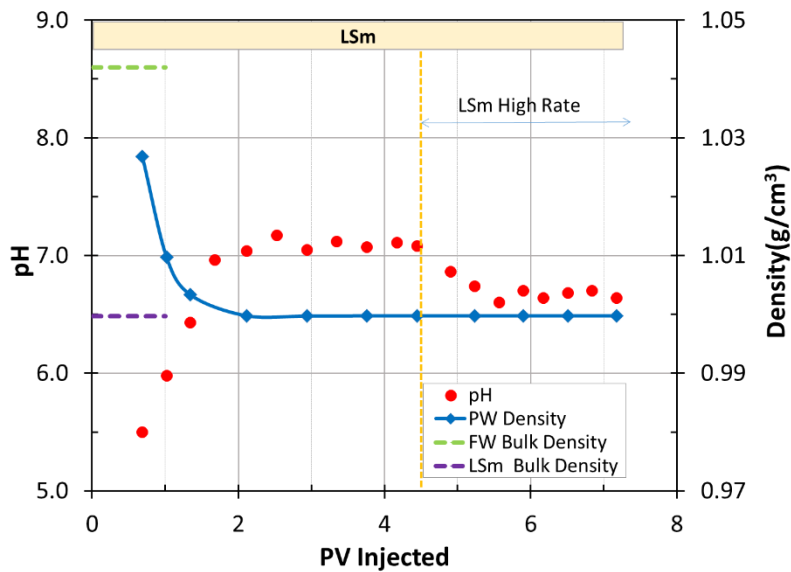


Figure 42. Produced water pH and density during oil recovery test on core-5 (1<sup>st</sup> restoration)

- **Ion Chromatography Analysis**

Figure 43 shows the concentration of calcium, magnesium, and sulfate from chemical analysis of the PW during first restoration of core-5. Generally, as more LSm is injected, the ions concentration decreases until it reaches the stable value.

As expected, during LSm flooding with injection rate 4 PV/D, the concentration of calcium dropped significantly from 35 mM to 1.2 mM as the transition from calcium rich formation water to the LSm which contained much less calcium. The stabilized concentration of calcium was 1.2 mM and it was higher than the bulk calcium concentration in LSm, 0.4 mM. Magnesium concentration rapidly reduced from 9 mM to the stable value, 0.27 mM. This stabilized concentration was lower than the bulk magnesium concentration of LSm, 0.67 mM as injected brine. Meanwhile sulfate concentration decreased gradually from 2.3 mM to 1.3 mM which was higher than the bulk sulfate concentration of LSm, 0.021 mM.

After the injection rate was increased to 16 PV/D, the calcium concentration slightly decreased to 0.8 mM, while magnesium concentration slightly increased to 0.32 mM, and sulfate concentration significantly decreased to 0.1 mM.

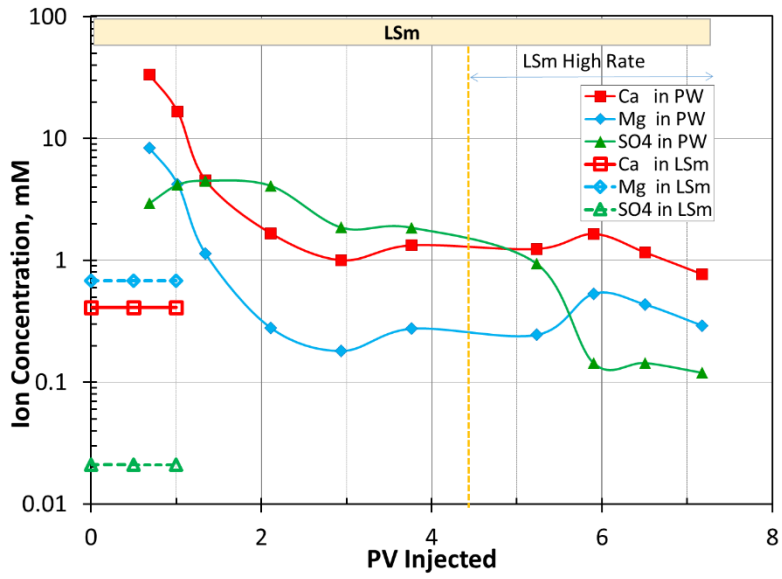


Figure 43. Ion chromatography analysis during oil recovery test on core-5 (1<sup>st</sup> restoration)

## 6 DISCUSSION

During the experiments, both core-3 and core-5 show excellent performances of low-salinity effect by significant extra oil produced. The main reason is that all the criteria for observing low salinity effects have been met. As discussed before, some criteria are required for the low-salinity to take effect, they are: clay must be present in the core (clay must be mixed-wet), active polar components must be present in the crude oil, and the formation water (FW) must contain divalent cations like  $\text{Ca}^{2+}$  and  $\text{Mg}^{2+}$ .

The cores contain clay. The formation water used in the experiments was high salinity brine (60,461 ppm) that had high concentration of  $\text{Na}^+$ , 929.8 mM, it also contains a significant amount of divalent cations, 44.2 mM of  $\text{Ca}^{2+}$  and 7mM of  $\text{Mg}^{2+}$ . Hence, when the core was 15 % saturated with FW, during preparations to the oil recovery experiment, the pH decreased and an acidic environment occurred (initial pH between 5.5 until 6.1). The low pH is necessary in order to obtain a high adsorption of polar components onto the clay surface when the core afterwards was saturated with oil.

The amount of acidic polar components in the crude oil is 0.16 mg KOH/g. Hence, there is a satisfied amount of polar components present in the crude oil. Previous low salinity flooding study showed that there appeared to be no restrictions to the type of polar components present in the crude oil, acids or bases, provided that a significant amount was present<sup>3</sup>. When oil is injected into the core, the polar components react with the formation water that already present in the core. The polar components takes protons,  $\text{H}^+$ , from the water and the affinity towards the negatively charge clay surface increased as illustrated before in equation 12 and 13 by an equilibrium movement to the left.



### 6.1 Oil Recovery

It has been mentioned earlier that these experiments are aimed to compare the production performance between SWm injection and LSm injection. On the other hand, the LSm injection is performed in secondary and tertiary mode. Figure 44 and Table 7 summarize the oil recovery performance from all experiments.

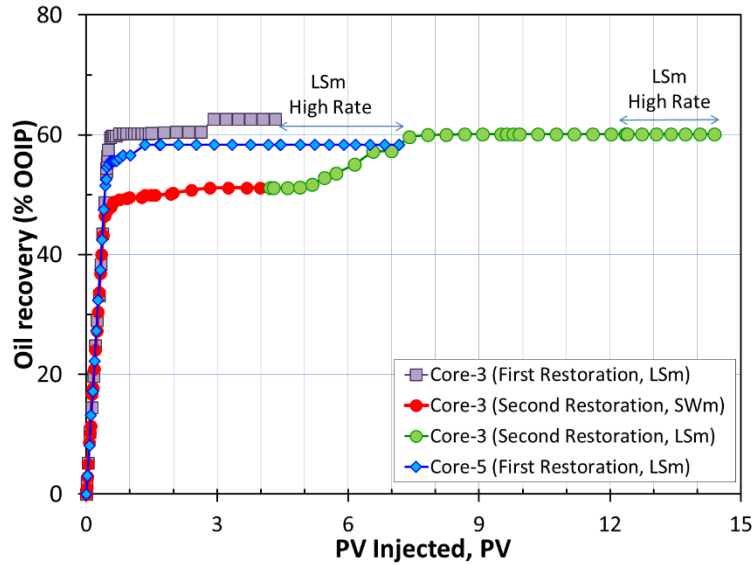


Figure 44. Comparison oil recovery for all experiments

Table 7. Breakthrough time and oil recovery for all experiments

Core & Restoration	Flooding Sequence	BT, PV Inj.	RF at BT, % OOIP	Secondary mode URF, % OOIP	Tertiary Mode URF, % OOIP
Core-3 (1 <sup>st</sup> )	LSm	0.46	53.9	62.6	no tertiary mode
Core-3 (2 <sup>nd</sup> )	SWm-LSm	0.42	47.0	51.2	60.1
Core-5 (1 <sup>st</sup> )	LSm	0.45	52.6	58.3	no tertiary mode

From Table 7, it is observed that in this study, LSm injection resulted in higher recovery than SWm injection. On the other hand, LSm injection gave benefit both in secondary and tertiary mode of flooding. From the first and second experiment when the same core was used, in the secondary mode sea water only produced 51% of OOIP while LSm could produce up to 63% of OOIP. SWm injection was also observed to have earlier water breakthrough (0.42 PV) compared to the LSm injection (0.46 PV). It indicated that LSm imbibes in small pore of the core and displaces the oil droplet resulted in delayed water breakthrough compared to SWm.

During oil recovery test on core-3 for the second restoration, the low salinity effect in the tertiary mode was observed obviously, after switching from SWm to LSm. The response time for observing low salinity effect was quite fast. It began to occur after injecting 0.5 PV of LSm. In this experiment, the second plateau was reached after injecting 3 PV of LSm which corresponded to add oil production about 9% of OOIP (51% compared to 60%).

When using relatively small cores during coreflood experiment, there is a possibility to observe end effect by increasing injection rate, especially when wettability

modifications are taking place. For both core-3 and core-5, the experiment results showed that there was no extra oil production was observed by increasing the flooding rate of LSm from 4 to 16 PV/D. It indicated that the amount of oil bank up at the end of the core was low.

Referring to Figure 44, the entire experiments show a similar slope of oil production before water breakthrough, it indicates core-3 and core-5 are homogeneous. After the water breakthrough, both of the cores were still able to produce oil which indicated mix-wet system in the cores. If the cores were water wet, the displacement process would behave as piston like displacement, thus no oil production observed after water breakthrough.

From the first and second experiment results, it is clear that the ultimate recovery from secondary mode of LSm flooding (62.6% of OOIP) is slightly higher than tertiary mode of LSm flooding (60.1% of OOIP). It could happened due to the change in initial wetting properties of the rock after the first experiment was done. The initial condition prior to the LSm injection was also different in the secondary and tertiary mode. In the secondary mode the initial brine in the core is formation water while in the tertiary mode is SWm.

The ultimate recovery from first experiment by using core-3 was slightly higher than ultimate recovery from third experiment by using core-5, even though both of the experiments were done in the secondary mode of low salinity waterflooding. It might be happen due to a slightly different composition of clay content and minerals effect.

SWm injection does not show significant smart water effect due to small pH increase (0.4 unit) from the initial pH of produced water. On the other hand, LSm injection shows that significant low-salinity effect due to significant pH increase (1.4 – 1.5 unit) from the initial pH. A significant pH increase promotes the desorption of polar oil compounds.<sup>3</sup>

## 6.2 pH Analysis

It has been mentioned earlier that clay surface is permanently negatively charged.  $\text{Ca}^{2+}$  ions that are attracted to this surface will create an equilibrium as presented in equation 11 previously:



From this chemical reaction, it can be concluded that injection of high salinity brine containing relatively high amount of  $\text{Ca}^{2+}$  ions will push the equilibrium to the left side, resulting in less pH increase. The injection of SWm brine resulted in an insignificant pH increase. During LSm in which contains very low amount of  $\text{Ca}^{2+}$ , the equilibrium will start move over to the right side and create  $\text{OH}^-$  ions that will increase the pH value.

In all of the experiments, initial pH of produced water came out at 5.5-6.16 pH units which indicate acidic environment equilibrium in the restored core. This matches with the evaluation by Austad et al.<sup>3</sup> for smart waterflooding to take any effect, which is acidic environment with pH range between 5 up to 6.5. In this pH range, high adsorption of polar organic compounds onto the clay will take place. The polar oil compound will attach to the clay surface and make the system more oil-wet. As low salinity brine is injected, the system becomes more water-wet due to the increase in pH and  $\text{H}^+$  ions will take sites on the clay surface, and release the oil compound. Finally the oil inside the cores is mobilized and increases the recovery factor.

The pH value of the first produced water which is actually displaced initial formation water usually represents reservoir initial pH. However in this project, the initial pH of the produced water was not fully caused by formation water, but also there was a small contribution of the injected brine (LSm or SWm). It can be seen from Table 4, both core-3 and core-5 have pore volume  $\sim 11.5$  ml and the initial water saturation is 15%, i.e. initial formation water volume is 1.65 ml. On the other hand, to be able to measure the pH, the volume of the produced water should be collected at least about 2.0 ml. So it can be concluded clearly that initial produced water consist of both FW and injected brines.

During the first restoration of core-3 and core-5, the initial produced water volume consisted of FW and LSm. On the other hand, for the second restoration of core-3 the initial produced water volume consisted of both FW and SWm. It was also supported by the initial effluent density from the first restoration of core-3 and core-5 was 1.025 gr/cc and second restoration of core-3 was 1.035 gr/cc, which was less than bulk formation water density (1.042 gr/cc).

It can be observed that pH increases significantly in the produced water during LSm injection from experiments' result. From the first restoration of core-3 and core-5 the pH increased about 1.4 – 1.5 pH unit in the secondary mode of LSm injection. This pH increase changed the COBR system from the acidic environment to alkaline environment.

In the second restoration of core-3 where the experiment was performed to evaluate SWm flooding in the secondary mode, the initial pH was 5.95, which indicated acidic

environment. During the SWm flooding, the pH number increased from 5.95 to 6.4 or only 0.4 pH increase from the initial pH. It shows that SWm injection can not change the equilibrium from acidic to alkaline condition. It means that SWm injection creates a buffering effect inside the core and smart water EOR will not take any effect.

In contrast, after switching from SWm to LSm flooding with constant injection rate of 4 PV/D, the pH of the PW increased significantly from 6.4 (the stable pH of SWm flooding) up to 7.8 and reached a plateau at pH 7.5. There was 1.5 pH unit differences in the pH number compared to the initial pH from produced water (5.95), which showed that LSm worked as smart water in the core. It showed that chemical reaction between crude oil, brine, and rock (COBR) had happened before the additional oil was being produced. This chemical reaction caused the mobilization of some oil during LSm flooding that could not be swept by SWm.

### **6.3 Ion Chromatography Analysis**

In this chapter the discussion will focus on the profile of calcium, magnesium, and sulfate concentration in produced water at injection rate 4 PV/D. Coreflood experiment results showed that higher injection rate, 16 PV/D, cannot mobilize any remaining oil in the cores. The stabilized concentration during injection rate 4 PV/D will be our main interest as no additional oil was produced during the high injection rate of 16 PV/D.

#### **6.3.1 Calcium**

From calcium ion concentration analysis, the first produced water sample which mainly contained FW had almost similar concentration with the bulk FW. The calcium concentration decreased as more as the SWm or LSm are injected. During SWm flooding in the second restoration of core-3, the stabilized calcium concentration of produced water was similar with the bulk concentration of SWm. The produced water concentration during LSm flooding for the first and second restoration of core-3 reached the bulk concentration of calcium in the LSm brine. It seemed there was no dissolution or precipitation of  $\text{Ca}^{2+}$  during the flooding process using core-3.

While for first restoration of core-5 the calcium concentration was higher almost twice than the bulk calcium concentration in LSm brine. It can be concluded that there is calcium dissolution from minerals in the core which are most likely anhydrite ( $\text{CaSO}_4$ ). Referring to the equation 11, the concentration of dissolvable salts like ( $\text{Ca}^{2+}$ ) can affect the exchange of active cations in the clay surface and pH.



Based on laboratory experiments by Aksulu et al.<sup>42</sup>, it is concluded that the presence of anhydrite in the reservoir will affect the LS EOR process. As the HS fluid is switched over to LS fluid, the solubility of the anhydrite present in the reservoir will increase. Refer to equation 21 the equilibrium will lean over to the left. It makes the relative replacing power of calcium stay high which prevents  $\text{Ca}^{2+}$  displacement by  $\text{H}^+$ , which finally will reduce the possibility desorption of polar organic compounds in the clay surface.



### 6.3.2 Magnesium

Another divalent cation that has been evaluated is magnesium. In the second restoration of core-3 for evaluating SWm flooding performance in the secondary mode, the magnesium concentration from first produced water was slightly higher than bulk concentration in the FW. It has been explained earlier that the first produced water contained not only FW but also some amount of SWm or LSm depending on the flooding process. The bulk magnesium concentration in the SWm was higher than FW. Thus, during the entire SWm flooding process, the magnesium concentration remained high.

After switching from SWm to LSm flooding, the magnesium concentration started to decrease and stabilized at a value much lower than the bulk concentration in the LSm. Similar results were also observed from the the first restoration of core-3 and core-5 where both of them were flooded using LSm in the secondary mode. Therefore  $\text{Mg}(\text{OH})_2$  precipitation might be occurred during the LSm flooding. Equation 22 shows the precipitation reaction of  $\text{Mg}(\text{OH})_2$ .



### 6.3.3 Sulfate

It was observed that there was a significant amount of sulfate, ranging from 0.3 mM to 0.4 mM from the first produced water in all three experiments, even though the displaced formation water did not contain any sulfate. At the end of LSm flooding process in the first restoration of core-3 and core-5 during injection rate 4PV/D, the sulfate concentration was 2 mM and 1.2 mM where the bulk sulfate concentration in

the LSm was only 0.021 mM. It could be an indication for dissolution of any dissolvable minerals containing  $\text{SO}_4^{2-}$ .

For core-5, anhydrite could be the sulfate minerals because at the end of LSm flooding process, it was also observed that higher concentration for  $\text{Ca}^{2+}$  in the produced water (1.3 mM) than the bulk concentration in the LSm, 0.4 mM. While for core-3, other sulfate minerals could dissolve because there was no increment in the stabilized calcium concentration of the produced water compared to the bulk calcium concentration of LSm during LSm flooding.

## 6.4 pH Screening Test

pH is an important factor of controlling the wetting condition of an oil reservoir. pH basically controls ion exchange that occurs in the reservoir between the oil and the clay surfaces. Adsorption of polar components in the crude oil towards the clay surfaces is highly determined by the pH number of its environment. The lower the pH, the higher the adsorption of the components on to the negative charged clays. These components basically act like anchor molecules that create a less water-wet rock surface. Low salinity water injection which usually higher in pH number, is an attempt to increase reservoir pH which eventually creates more water-wet environment. The so called Low Salinity effect that has been observed in sandstone reservoirs creates wettability alteration towards more water wet condition that may induce positive capillary pressure and improve microscopic sweep efficiency.

Zahra Aghaeifar, a Ph.D student at University of Stavanger has conducted pH screening to observe the interaction between the minerals present in the reservoir core and the brines which are formation water (FW), modified sea water (SWm) and smart water/modified low salinity brine (LSm). The interaction is indicated by the pH changes throughout the experiments. pH screening test provides valuable information to evaluate smart water which might be potentially applicable in the observed reservoir. In the pH screening test core-4 was used, taken from the same reservoir with core-3 and core-5.

Prior the test, core-4 was initially cleaned, restored and dried. The core was then completely 100% saturated with formation water. Afterwards, it was flooded with FW, SWm and LSm at a constant injection rate, 4PV/D. For each brine, the flooding was performed until stable pH and water density have been reached. The experiment was performed at three different temperatures, 136°C, 100°C and 70°C. In this thesis the result will be presented only for temperature 136°C as shown in figure 43.

The test was performed by injecting the brines in a constant rate of 4 PV/D. As shown in the Figure 45, the flooding sequence is FW-SWm-LSm-FW-LSm-FW. The initial pH during the first FW flooding is at 7.0 and is getting stable at about 7.3. When it is followed by the SWm flooding, the pH number does not give significant changes and remains at 7.3. The increase in pH number occurs in the LSm zone, in which the pH is stable at 8. During the second FW flooding, the pH decreases to 6.8 and rises back up to 8.2 in the second LSm injection.

As shown in the previous chapter, the initial pH obtained from the test is different with the ones gathered from both Core-3 and 5. This has happened because both cores were used for flooding process and initially saturated with water and oil that resulted in lower initial pH. It can be noticed from this test that pH increase from sea water flooding was only about 0.4 pH unit whereas increase from flooding using LSm brine could be up to 1.0 pH unit. The pH increase result confirms that SWm does not give significant low salinity effect while LSm gives better low salinity effect. The pH increments are consistent with the ultimate oil recoveries using SWm or LSm.

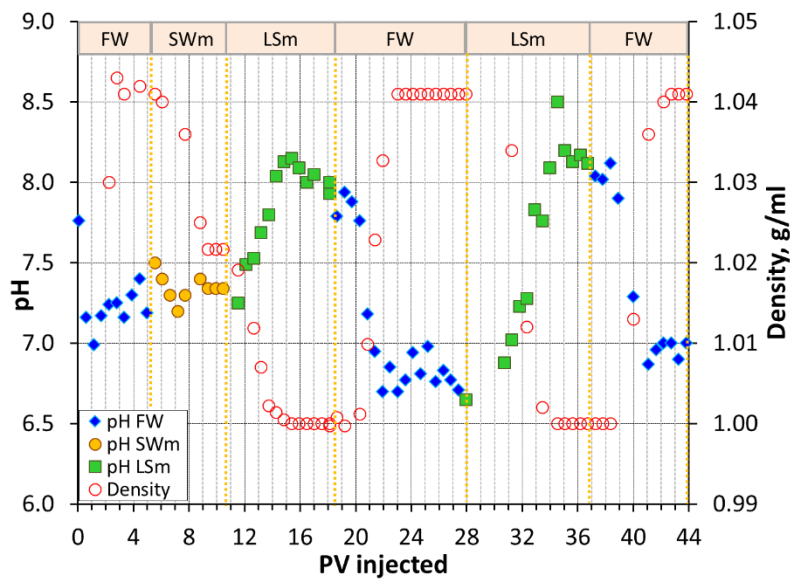


Figure 45. pH screening test of core-4 at 136°C<sup>48</sup>

## 6.5 Temperature and Formation Water Salinity Effect

Basic and acidic organic materials of crude oil can be adsorbed onto the negative sites of clay surface. This adsorption is affected by three essential factors: reservoir pH, temperature, and salinity or ion composition of the formation water. Polar organic materials will compete with the active cations present in the water in order to make a

reaction with the negative sites of the clay. The reaction later will determine initial wetting condition of the reservoir. Fundamentally, when the cations succeed to react with the negative site, the reservoir will tend to be water-wet; otherwise if the adsorption of oil molecules is more predominant, an oil-wet reservoir will likely exist.

Temperature also plays a significant role as it affects ion solubility within the water that will determine the reactivity of the water towards the rock surface. For instance, temperature changes will affect desorption process of  $\text{Ca}^{2+}$  from clay surface as the reaction is exothermic; temperature increase will also decrease the low-salinity effect due to a low pH gradient. The chemical reaction can be explained by equation 11.



Increase in temperature will move the reaction from right to left of which resulting in decrease of  $\Delta\text{pH}$ . For short, increase in temperature and salinity will reduce the amount of polar components adsorbed on the clay surface, thus decreasing the potential for low-salinity EOR (LS EOR) to take effect. However, in this study, significant LS EOR effect occurred at high temperature,  $136^\circ\text{C}$ , after switching from SW to LS flooding. This likely happened because relatively low salinity of formation water (60,461 ppm) existed at that high temperature. Therefore, low salinity environment pushed the reaction from left to right and reduced  $\text{Ca}^{2+}$  desorption resulting in a higher pH gradient.

Aghaeifar et al.<sup>47</sup> have previously conducted a study with slightly similar environment. The LS EOR potential was studied at  $110^\circ\text{C}$  by using different formation water salinity. Two preserved reservoir cores were used and assumed to share identical physical and chemical properties. The first core was saturated with relatively high salinity formation water about 200,000 ppm. The flooding sequence was FW (200,000 ppm)-SW (33,000 ppm) -LS (660 ppm). No LS EOR effect was observed during SW and LS brine flooding. Core saturated with formation water with high  $\text{Ca}^{2+}$  concentration might appear too water wet for observing LS EOR effects even though the clay content is relatively enough and the crude oil contains significant amounts of polar components. For the second core, formation water used during the experiment was 23,000 ppm. As expected, there was no pH increase and extra oil produced after switching from 23,000 ppm of FW to 33,000 ppm of SW. However, significant increase in oil recovery almost 6% of OOIP and pH increase about 1.5 pH units occurred when switching from SW to LS of which the process triggered wettability alteration and LS EOR effect.

In summary, based on the results obtained from the author's experiments and references from previous study experiences, it can be concluded that at high temperature ( $>100^\circ\text{C}$ ) with high salinity FW, reservoir behaves too water wet then it will

hard to see LS EOR effect, but using lower salinity of FW which leads to mixed wet initial condition and increases LS EOR potential. The results from this thesis confirm the salinity of FW used in this project (60,461 ppm) is low enough to see LS EOR effect.

## 6.6 Viability of Smart Water Fluids

It has been mentioned before that SW that was used in this project does not have the real sea water composition. SWm was made from the sea water which is depleted in  $\text{SO}_4^{2-}$  to prevent scaling problem due to presence of barium ( $\text{Ba}^{2+}$ ) and strontium ( $\text{Sr}^{2+}$ ) in the formation water. The LSm was made by diluting SWm twenty times. That means, there will be additional cost to make both SWm by filtration and LSm by dilution of SWm, but still making LS brine is much cheaper than the other EOR methods. On the other hand, core flooding experiments show that LSm injection can increase oil production about 11% of OOIP or 22% of total oil production compare to SWm injection. Significant increment of recovery can compensate the initial cost needed to make LSm. Detail economical evaluation has to be done to know how much the profit is.

In this project, experiments have been performed in one dimension and show good LS EOR effect. So to confirm the result for real reservoir condition, we need to upscale the setup and do the experiment and reservoir simulation in two or three dimension displacement.

Secombe et al.<sup>49</sup> have carried out a study modeling smart water in enhancing oil recovery. They used commercial software and laboratory experiment to simulate smart water slug injection in a one-dimensional model. The software simulation indicated that only 40% PV of the brine was required to get the smart water effect for the entire reservoir. This amount of water was said to be adequate to overcome salinity problems caused by diffusion between the injection brine and the existing formation water in the reservoir. Similar indication was also found from the core experiment which could also be considered as a one-dimensional model to support their software simulation result.

However, some criticized that the result became too optimistic if compared to two-dimensional 5-spot models. It is because, if the 40% PV injection was applied to a two-dimensional-5-spot model, the oil increase would significantly be much lower than what it was discovered in the one-dimensional model. It is also suggested that larger slug size would be required to overcome diffusion problems.

Effectiveness of an EOR method to improve oil production can be evaluated from its macroscopic and microscopic efficiencies. In regards to smart water technology,

understanding the diffusion characteristics of the reservoir is essential as this will affect the microscopic efficiency. Diffusivity will dictate the salinity gradient and determine the slug size volume needed to ensure that the complete reservoir will benefit from the Smart Water flooding. Then, a comprehensive model is required for simulating the displacement process in the reservoir.

Macroscopic sweep efficiency depends on the effectiveness of the displacing fluid in contacting the reservoir in taking out the volume of reservoir, both areally and vertically. As shown before in Figure 46, there will be some unswept area left behind the displacement front. That is why three-dimensional model is considered to be more representative to simulate the displacement process in reservoir rather than the one-dimensional model. A reservoir model built using commercial software is important not only to understand how the smart water affects the entire field but also to predict how much oil will be produced which may affect the economical aspect of the project.

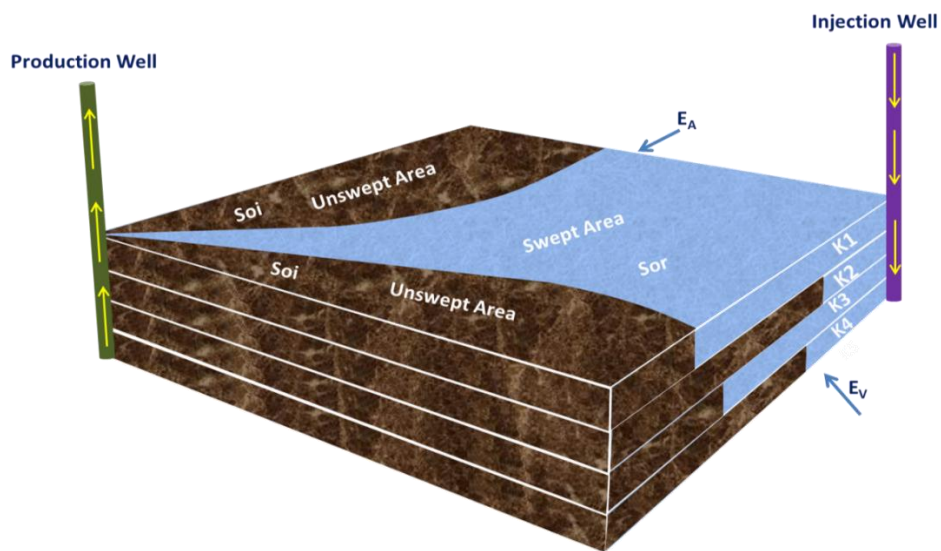


**Figure 46. Macroscopic/volumetric sweep efficiency illustration (areal and vertical) in a three-dimensional model**

Therefore, a more comprehensive experimental, simulation studies, and pilot testing are necessary before implementing smart water for field scale projects. Pilot test in the BP Endicott field in Alaska has shown promising results.<sup>50</sup> The incremental oil recovery is equal to 10% of the total pore volume in the swept area after 1.3 PV of low salinity brine was injected. In 2016, BP will start to apply for the first field scale implementation of low salinity waterflooding at Clair Ridge Field in UK by expecting additional reserves around 42 million barrels oil. The additional lifting cost is only 3\$/barrel, much cheaper than the other EOR technique about 20\$/barrel.<sup>26</sup> This lifting cost shows that low salinity/smart waterflooding is still able to generate profit, even at low oil price.

## 7 CONCLUSION

A series of experiments were performed to test low salinity effects in three sandstone reservoir cores. Modified sea water (SWm) 30,122 ppm and modified low saline water (LSm) 1,538 ppm were flooded in the oil recovery test. All the cores were aged and flooded at 136°C. A pH-screening test was successfully flooded with formation water (FW), SWm, and LSm at 136°C. Based on the results and discussions, the following points can be concluded:

- Low salinity brine injection (LSm) gives higher recovery than sea water (SWm) injection in the secondary mode; ultimate oil recovery by LSm is 63% of OOIP while for SWm injection is 51% of OOIP.
- After SWm injection, it is observed that low salinity effect in tertiary mode injection gives an extra recovery of 9% of OOIP.
- About 1.5 pH unit increase in pH and changing from acidic environment to alkaline environment were observed when FW was displaced by LSm, which is in line with the LS EOR mechanism that has been proposed by Austad et al.<sup>3</sup>, desorption of polar oil components due to pH increase which come to wettability alteration on the rock surface in the crude oil-brine-rock (COBR) system.
- SWm injection is unable to create smart water effect in the given COBR systems. The insignificant pH increase (0.4 pH unit) indicates buffering effect in the system during SWm injection.
- pH changes during the oil recovery tests are consistent with pH changes in previously performed pH screening test without oil present.

## 8 FUTURE WORK

Based on experimental findings presented in this thesis, below are several recommendations for future works which will be useful for EOR team at the University of Stavanger:

1. Core -5 has to be restored for the second time and flooded with SWm followed by LSm to compare it with core-3 experiment's result.
2. New cores should be flooded with SWm injection in secondary mode followed with LSm after SWm for the first restoration. Later on, reuse the cores for the second restoration and flood it directly with LSm in secondary mode.
3. Mineralogy of the core materials have to be clarified by XRD analysis to be able to discuss more about the results.
4. Upscaling of the results using 2D and 3D models.

## REFERENCES

1. BP. Energy Outlook 2035. [online] Available at <<http://www.bp.com/en/global/corporate/about-bp/energy-economics/energy-outlook.html>> . 2015. [Accessed date: 11 March 2015]
2. Schumacher, M.M. Enhanced Oil Recovery : Secondary and Tertiary Method. Noyes Data Corp, Park Ridge, New Jersey. Chapter 2 : 18-23.1978
3. Austad, T.; RezaeiDoust, A.; Puntervold, T. Chemical Mechanism of Low Salinity Water Flooding in Sandstone Reservoirs. Paper SPE 129767 presented at the 2010 SPE Improved Oil Recovery Symposium held in Tulsa, Oklahoma, USA, 24-28 April 2010.
4. Puntervold, T. Waterflooding of carbonate reservoirs - EOR by wettability alteration. PhD Thesis, University of Stavanger. 2008
5. Cuong, T.Q.D; Long X.N., Zhangxin, C; Quoc, P.N. Modeling Low Salinity Waterflooding: Ion Exchange, Geochemistry and Wettability Alteration. SPE Paper 166447, presented at SPE Annual Technical Conference and Exhibition held in New Orleans, Louisiana, USA, 30 September -2 October 2013.
6. Zolotukhin, A.B.; Ursin, J.R. Introduction to Petroleum Reservoir Engineering. Kristiansand: Høyskoleforlaget. 2000.
7. Nedeau, P.H.; Ehrenberg, S.N. Sandstone vs. carbonate petroleum reservoirs: A global perspective on porosity-depth and porosity-permeability relationships. The American Association of Petroleum Geologists. 2005.
8. IDF. Clay Chemistry. Technical Manual for Drilling, Completion and Workover Fluids. International Fluids Limited.1982
9. Morad, S.; Worden, R.H. Clay mineral cement in sandstones. Specil publication of International Association of Sedimentologist Blackwell. 2003.
10. Tang, G.; Morrow, N. R. Oil Recovery by Waterflooding and Imbibition – Invading Brine Cation Valency and Salinity. Paper SCA9911.1999.
11. Jerauld, G.R.; Lin, C.Y.; Webb, K.J.; Seccombe, J.C. Modelling Low-Salinity Waterflooding. Paper SPE 102239, presented at the 2006 SPE Annual Technical Conference and Exhibition held in San Antonio, Texas, USA, 24-27 September. 2006.
12. Boussour, S.; Cissokho, M.; Cordier, P. ; Bertin, H.; Hamon, G. Oil Recovery by Low Salinity Brine Injection: Laboratory Results in Outcrop and Reservoir Cores. Paper SPE 124277, presented at the 2009 SPE Annual Technical Conference and Exhibition held in New Orleans, Louisiana, USA, 4-7 October 2009.
13. Green, D.W; Willhite, G. P. Enhanced Oil Recovery. SPE textbook series, 6. Henry L. Doherty Memorial Fund of AIME Soceity of Petroleum Engineers, Richardson, TX USA. 1998.

14. Ela, M.A.E; Sayyoub, H; Tayeb, E.S.E. An integrated approach for the application of the Enhanced Oil Recovery Projects. Journal of Petroleum Science Research (JPSR) volume 3, issue 4, October 2014.
15. Anderson, W. Wettability literature survey-part 2: Wettability measurement. Journal of Petroleum Technology, 38(11), 1,246-241,262. 1986.
16. Strand, S. Wettability alteration in chalk - A study of surface chemistry. Dr.Ing. Thesis, University of Stavanger, Dr. Ing. Thesis. 2005.
17. Treiber, L.E; Archer, D; Owens, W.W. A laboratory evaluation of the wettability of fifty oil-producing reservoirs. Society of Petroleum Engineers Journal. 1972.
18. Skauge, A., and Ottesen, B. A Summary of Experimentally Derived Relative Permeability and Residual Saturation on North Sea Reservoir Cores. Reviewed Proceeding from the 2002 International Symposium of the Society of Core Analysts (SCA), held in , Monterey, California, USA, 22-25 September 2002.
19. Bernard, G.G. Effect of floodwater salinity on Recovery Of Oil from Cores Containing Clays, SPE California Regional Meeting. 1967.
20. Lager A., W.K.J., Black C. J. J. Impact of Brine Chemistry on Oil Recovery. Paper A24 presented at the 14<sup>th</sup> European Symposium on Improved Oil Recovery, Cairo, Egypt, 22-24 April. 2007
21. Suijkerbuijk, B. M. J. M.; Sorop, T. G.; Parker, A. R.; Masalmeh, S. K.; Chmuzh, I. V.; Karpan, V. M.; Volokitin, Y. E.; Skripkin, A. G. Low Salinity Waterflooding at West Salym: Laboratory Experiments and Field Forecasts. SPE Paper 169691, presented at 2014 SPE EOR Conference at Oil and Gas West Asia, Muscat, Oman, 31 March – 2 April. 2014.
22. Strand, S; Austad, T; Puntervold, T; Aksulu, H; Haaland, B; RezaeiDoust, A. Impact of Plagioclase on the Low Salinity EOR-Effect in Sandstone. Energy Fuels 28: 2378-2383. 2014.
23. Yousef, A.; Liu, J.; Blanchard, G.; Al-Saleh, S.; Al-Zahrani, T.; Al-Zahrani, R. ; Al-Tammar, H. ; Al-Mulhim, N. SmartWater Flooding: Industry's First Test in Carbonate Reservoir. SPE 159526, presented at SPE Annual Technical Conference and Exhibition held in San Antonio, Texas, USA. 8-10 October 2012.
24. Skrettingland, K; Holt, T; Tveheyo, M.T; Skjevrak. 2011. Snorre Low Salinity-Water Injection-Coreflooding Experiments and Single-Well Field Pilot. SPE Paper SPE 129877, presented at SPE Improved Oil Recovery Symposium, Tulsa 24-28 April, Tulsa, Oklahoma, USA. 2011.
25. Webb, K.J. ; Black, C.J.J. ; Al-Ajeel. Low Salinity Oil Recovery-Log-Inject-Log. Paper SPE 89379, presented at SPE Symposium on Improved Oil Recovery, Tulsa, 17-21 April 2004.
26. BP. 2015. Low Salinity Water Bring Awards For BP. Available at <<http://www.bp.com/en/global/corporate/press/bp->

magazine/innovations/offshore-technology-award-for-clair-ridge.html>

[Accessed date: 02 March 2015]

27. Zhang, Y; Morrow, N.R. Comparison of Secondary and Tertiary Recovery with Change in Injection Brine Composition for Crude Oil/Sandstone Combinations. Paper SPE 99757, presented at the SPE Improved Oil Recovery Meeting, held in Tulsa, Oklahoma, April, 2006.
28. Reinholdtsen, A. J.; RezaeiDoust, A.; Strand, S.; Austad, T. In Why such a small low salinity EOR - potential from the Snorre formation?16<sup>th</sup> European Symposium on Improved Oil Recovery, Cambridge, UK, 12–14 April, 2011.
29. Tang, G ; Morrow N.R. Influence of brine composition and fine migration on crude oil/brine/rock interactions and oil recovery. Journal Petroleum Science and Engineering. 24:99-111. 1999.
30. Strand, S; Puntervold, T. Introduction of Smart Waterflooding. Class presentation at University of Stavanger. 2015.
31. Strandnes, D.C. Enhanced Oil Recovery from Oil-wet Carbonate Rock by Spontaneous Imbibition of Aqueous Surfactant Solutions. PhD thesis Stavanger. 2008.
32. Buckley, J.S. ; Liu, Y. ; Monsterleet, S. Mechanisms of Wetting Alteration by Crude Oils. SPE Journal, 3(1): 54-61. 1998.
33. Secombe, J.C.; Lager, A. ; Webb, K. ; Jerauld, G. ; Fueg, E. Improving Waterflood Recovery: LoSalTM EOR Field Evaluation. SPE Paper 113480, presented at SPE/DOE Improved Oil Recovery Symposium held in Tulsa, Oklahoma, USA, 19-23 April 2008.
34. RezaeiDoust, A. Low Salinity Water Flooding in Sandstone Reservoir. PhD Thesis. University of Stavanger. 2011.
35. Tang, G.-Q. Brine Composition and Waterflood Recovery for selected Crude Oil/Brine/Rock Systems, PhD thesis, University of Wyoming, Laramie. 1998.
36. Mc Guire, P.L., Chatham, J. R., Paskvan, F. K., Sommer, D.M., Carini, F. H. Low Salinity Oil Recovery: An Exciting New EOR Opportunity for Alaska's North Slope. SPE Paper 93903, presented at the 2005 Western Regional Meeting held in Irvine, CA, USA, 30 March - 1 April. 2005.
37. Boussour, S., Cissokho, M., Cordier, P., Bertin, H., Hamon, G. Oil Recovery by Low Salinity Brine Injection: Laboratory Results in Outcrop and Reservoir Cores. Paper SPE 124277, presented at the 2009 SPE Annual Technical Conference and Exhibition held in New Orleans, Louisiana, USA, 4-7 October. 2009.
38. Lager A., W.K.J., Black C. J. J., Singleton M., Sorbie K. S. Low Salinity Oil Recovery - An experimental investigation. Paper SCA2006-36, presented at the International Symposium of the Society of Core Analysts held in Trondheim, Norway 12-16 September. 2006.

39. Ligthelm, D.J. Novel Waterflooding Strategy By Manipulation Of Injection Brine Composition, EUROPEC/EAGE Conference and Exhibition. Society of Petroleum Engineers, Amsterdam, The Netherlands. 2009.
40. RezaeiDoust, A. ; Puntervold T. ; Strand S. ; Austad T. Smart Water as Wettability Modifier in Carbonate and Sandstone: A Discussion of Similarities/Differences in the Chemical Mechanisms. *Energy & Fuels*, 23(9): 4479-4485. 2009.
41. Strand, S. Personal Discussion. University of Stavanger. 2015
42. Aksulu,H., Håmsø, D., Strand, S., Puntervold, T., and Austad, T. Evaluation of low-salinity enhanced oil recovery effects in sandstone: Effects of the temperature and pH gradient. *Energy & Fuels*, Vol. 26, 2012.
43. Fjelde,I. ; Aasen, S.M. ; Omekeh, A. Low salinity waterflooding experiments and interpretation. SPE Paper 154142, presented at SPE symposium on Improved Oil Recovery, 14-15 April, Tulsa, Oklahoma, USA, 2012.
44. Winoto, W. ; Loahardjo ; Xie,X.S; Secondary and Tertiary Recovery of Cruid Oil from Outcrop and Reservoir Rocks by Low Salinity Waterflooding. SPE 154209.2012.
45. Skrettingland, K. ; Holt, T. ; Tweheyo, M.T. ; Skjevraak, I. Snorre Low Salinity Water Injection - Core Flooding Experiments And Single Well Field Pilot. SPE Paper 129877, presented at SPE Improved Oil Recovery Symposium. Society of Petroleum Engineers,Tulsa, Oklahoma, USA. 2010.
46. Quan, X. ; Qingjie, L. ; Desheng, M. ; Jiazhong, W. Influence of brine composition on C/B/R interactions and oil recovery in low permeability reservoir cores, The 33<sup>rd</sup> annual IEA EOR conference and symposium, Regina, Canada, 27-30 August 2012.
47. Aghaeifar, Z; Strand, S; Austad, T; Puntervorld, T; Storås, S. The Influence of the Formation Water Salinity on the Low Salinity EOR-effect in Sandstone at High Temperature. 77<sup>th</sup> EAGE Conference & Exhibition 2015. Madrid IFEMA, Spain, 1-4 June 2015.
48. Aghaeifar, Z; Puntervorld, T; Strand, S; Austad, T. Unpublished Paper. 2015.
49. Seccombe,J.; Lager, A, Webb, K, Jerauld, G, and Fueg, E. Improving waterflood recovery: LoSal™ EOR Field Evaluation. Paper SPE 113480, presented at SPE/DOE Symposium on Improved Oil Recovery, 19-23 April, Tulsa, Oklahoma, USA. 2008.
50. Seccombe, J. ; Lager, A. ; Jerauld, G ; Jhaveri, B. ; Buikema, T. ; Bassler, S ; Denis, J. ; Webb, K. ; Cockin, A. ; Fueg, E. ; Paskvan, F. Demonstration of Low Salinty EOR at Interwell Scale, Endicott Field, Alaska. Paper SPE 129692, presented at the 2010 SPE Improved Oil Recovery Symposium held in Tulsa, Oklahoma USA, 24-28 April 2010.

## **SYMBOLS AND ABBREVIATIONS**

$\theta$	Contact angle, $^{\circ}$
$\Delta\rho$	Density difference between oil and water, $\text{g/cm}^3$
$\rho_{\text{DFW}}$	Density of diluted FW, $\text{g/cm}^3$
$\sigma_{\text{ow}}$	Interfacial tension oil-water, $\text{mN/m}$
$\Delta P$	Pressure across capillary tube
$\bar{v}$	Average velocity in capillary tube, $\text{m/s}$
$\mu_o$	Oil viscosity, $\text{cp}$
$\mu_w$	Water viscosity, $\text{cp}$
A	Cross section area of core, $\text{m}^2$
AN	Acid number, $\text{mg KOH/g oil}$
BN	Base number, $\text{mg KOH/g oil}$
BPV	Back pressure valve
COBR	Crude, oil, brine, and rock
D	Core diameter, $\text{cm}$
DI	Deionized water
$E_d$	Microscopic sweep efficiency
$E_M$	Macroscopic sweep efficiency
EOR	Enhanced oil recovery
$E_T$	Total displacement efficiency
$F_c$	Capillary force
$F_v$	Viscous force
FW	Formation water
g	Acceleration due to gravity, $\text{m/s}^2$
$g_c$	Conversion factor, 32.174
h	Height of the liquid column, $\text{m}$
HS	High salinity
IC	Ion chromatography
IOR	Improved oil recovery
K	Absolute permeability, $\text{mD}$
$K_{ro}$	Relative permeability of oil
$K_{rw}$	Relative permeability of water
L	Core length, $\text{cm}$
LS	Low salinity
LSm	Modified low salinity brine
M	Mobility ratio
n	Dilution degree

$N_{ca}$	Dimensionless capillary number
NW	Neutral wet
OOIP	Original oil in place, ml
$P_c$	Capillary pressure, Pa
$P_o$	Oil-phase pressure at a point just above the oil-water interface
PV	Pore volume, $cm^3$
$P_w$	Water-phase pressure just below the interface
PW	Produced water
Q	Volumetric flow rate, $m/s^3$
r	Radius cylindrical pore channel, m
RF	Recovery factor, %
$S_{or}$	Residual oil saturation, %
SOW	Strongly oil wet
SW	Sea water
SWm	Modified sea water
$S_{wi}$	Residual water saturation, %
SWW	Strongly water wet
TDS	Total dissolved solid, g/l
v	Interstitial pore velocity
$V_p$	Cumulative oil produced, ml
$W_d$	Weight of dry core, g
$W_s$	Weight of core 100% saturated with diluted FW, g

## APPENDICES

### A.1 AN and BN Measurement

The procedure used is listed below:

1. Calibrate the pH electrode with standard buffer solution with pH 4, 7 and 10.
2. Standardize the titrant with 50 ml of standard solution.
3. Make a sample of 1 ml spiking solution and 50 ml blank solution (made by using titration solvent). To improve the accuracy of the measurements of oils that have low AN, the spiking solution is added. Titrant is used to measure the total acid/base content of the sample.
4. Make a new sample of 1 ml spiking solution and 50 ml blank solution, and add 1 ml oil to the mixture. Use the titrant to measure the total acid/base content of the new sample.
5. The amount of oil added is represented by the difference in the total acid/base content between the blank and the sample containing oil.

### A.2 Viscosity Measurement

The procedure on how to conduct the measurement is listed as followed:

1. The instrument accuracy has to be tested with deionized water. 2.2 ml of the water is placed on the metal plates.
2. Put the instrument on the measuring position with the plates close to each other.
3. Make sure that the plates are fully filled with the liquid. Put some more liquid if necessary.
4. Set the shear rates between 100 and 600  $s^{-1}$ . Measure the shear stress, write down the reading for each shear rate value.
5. Draw a curve of which the shear rate and shear stress are on the X and Y axes, respectively.
6. The fluid viscosity can be calculated from the area below the linear slope of the curve.
7. Repeat the measurement few more times until the desired accuracy is achieved.

### A.3 Ion Chromatography

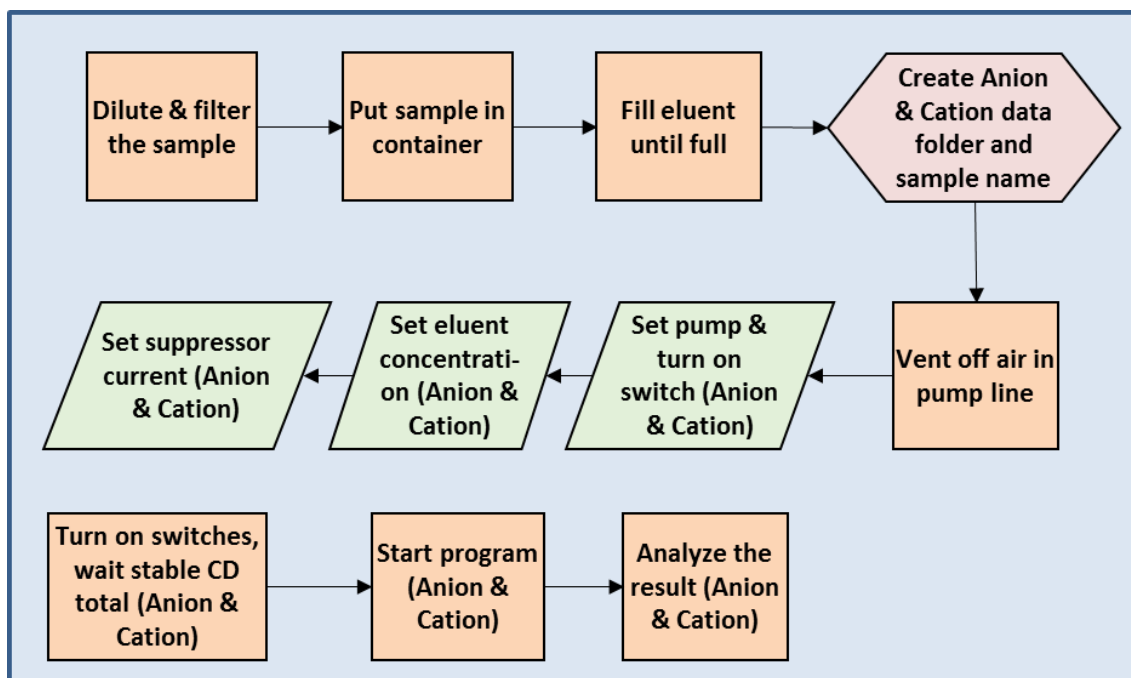


Figure A-1. Flowchart of Ion Chromatography experiment

During oil recovery test, collect the brine water in bottle sample. Then, measure the Cation and Anion concentration on the sample by Ion Chromatography method using Dionex ICS-300. Figure A-1 shows the flowchart of Ion Chromatography experiment. Detailed steps are described as follow.

1. Dilute and filter the sample

The first step in Ion Chromatography method is to dilute the sample 500 times and filter it through 0.2  $\mu\text{m}$  filter using Gilson GX-271. The sample needs to be diluted and filtered to get optimum detection in ion chromatography method.

2. Put sample in container

The next step is to put effluent sample bottle in sample container. Put the sample in the container according to the position (1-100) which will be specified in the data list through the software program. Beside effluent sample, it is very important to put reference sample with known composition in the sample container.



**Figure A-2. The position of the samples in the sampler of IC system**

3. Fill eluent until full

The next preparation step is to fill eluent DI (deionized water) container until full for both Anion and Cation bottle (Figure A-3). The eluent function is to carry brine sample through resin.



**Figure A-3. The containers of anion and cation eluent DI water**

4. Create data folder & sample

The next step is to create separate data files for each Anion and Cation experiment (Figure A-4). On each data file, edit the “name column” and “position column” according to the position of effluent in the sample container.

#	CD	Name	Type	Level	Position	Volume [µl]	Instrument Method
1	Loading	mPW 1.500	Unknown		RB4	2.5	0.25 Row10 mM MSA 8 mA current 16 min analysis time CS19-4up
2	Loading	mPW 1.500	Unknown		RB4	2.5	0.25 Row10 mM MSA 8 mA current 16 min analysis time CS19-4up
3	Loading	mSW 1.200	Unknown		RD1	2.5	0.25 Row10 mM MSA 8 mA current 16 min analysis time CS19-4up
4	Loading	mSW 1.200	Unknown		RD1	2.5	0.25 Row10 mM MSA 8 mA current 16 min analysis time CS19-4up
5	Loading	mSW 1.200	Unknown		RE1	2.5	0.25 Row10 mM MSA 8 mA current 16 min analysis time CS19-4up
6	Loading	mSW 1.200	Unknown		RE1	2.5	0.25 Row10 mM MSA 8 mA current 16 min analysis time CS19-4up
7	Loading	mLS 1.200	Unknown		RC5	2.5	0.25 Row10 mM MSA 8 mA current 16 min analysis time CS19-4up
8	Loading	mLS 1.200	Unknown		RC5	2.5	0.25 Row10 mM MSA 8 mA current 16 min analysis time CS19-4up
9	Loading	1.1200	Unknown		RA1	2.5	0.25 Row10 mM MSA 8 mA current 16 min analysis time CS19-4up
10	Loading	2	Unknown		RA2	2.5	0.25 Row10 mM MSA 8 mA current 16 min analysis time CS19-4up
11	Loading	3	Unknown		RA3	2.5	0.25 Row10 mM MSA 8 mA current 16 min analysis time CS19-4up
12	Loading	5	Unknown		RA4	2.5	0.25 Row10 mM MSA 8 mA current 16 min analysis time CS19-4up
13	Loading	7	Unknown		RA5	2.5	0.25 Row10 mM MSA 8 mA current 16 min analysis time CS19-4up
14	Loading	9	Unknown		RA6	2.5	0.25 Row10 mM MSA 8 mA current 16 min analysis time CS19-4up
15	Loading	11	Unknown		RA7	2.5	0.25 Row10 mM MSA 8 mA current 16 min analysis time CS19-4up
16	Loading	13	Unknown		RA8	2.5	0.25 Row10 mM MSA 8 mA current 16 min analysis time CS19-4up
17	Loading	15	Unknown		RB1	2.5	0.25 Row10 mM MSA 8 mA current 16 min analysis time CS19-4up
18	Loading	17	Unknown		RB2	2.5	0.25 Row10 mM MSA 8 mA current 16 min analysis time CS19-4up
19	Loading	19	Unknown		RB3	2.5	0.25 Row10 mM MSA 8 mA current 16 min analysis time CS19-4up
20	Loading	mSW 1.200	Unknown		RE2	2.5	0.25 Row10 mM MSA 8 mA current 16 min analysis time CS19-4up
21	Loading	mSW 1.200	Unknown		RE2	2.5	0.25 Row10 mM MSA 8 mA current 16 min analysis time CS19-4up
22	Loading	mLS 1.200	Unknown		RC5	2.5	0.25 Row10 mM MSA 8 mA current 16 min analysis time CS19-4up
23	Loading	mLS 1.200	Unknown		RC6	2.5	0.25 Row10 mM MSA 8 mA current 16 min analysis time CS19-4up

Figure A-4. An example of the list of sample data, containing their names and positions in the sampler

5. Vent off air in pump line

The next step is to vent air from pump line by 1/2 turning priming knob on each Anion & Cation line (Figure A-5).

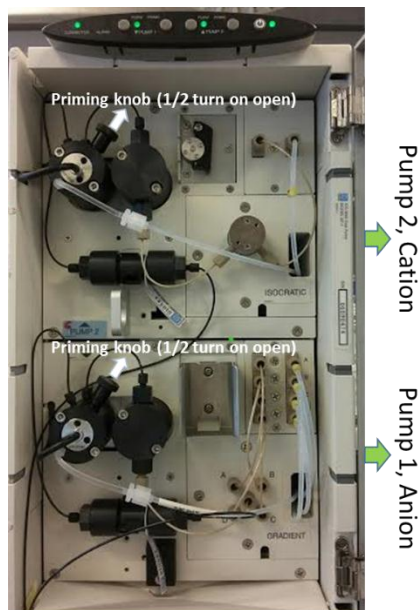
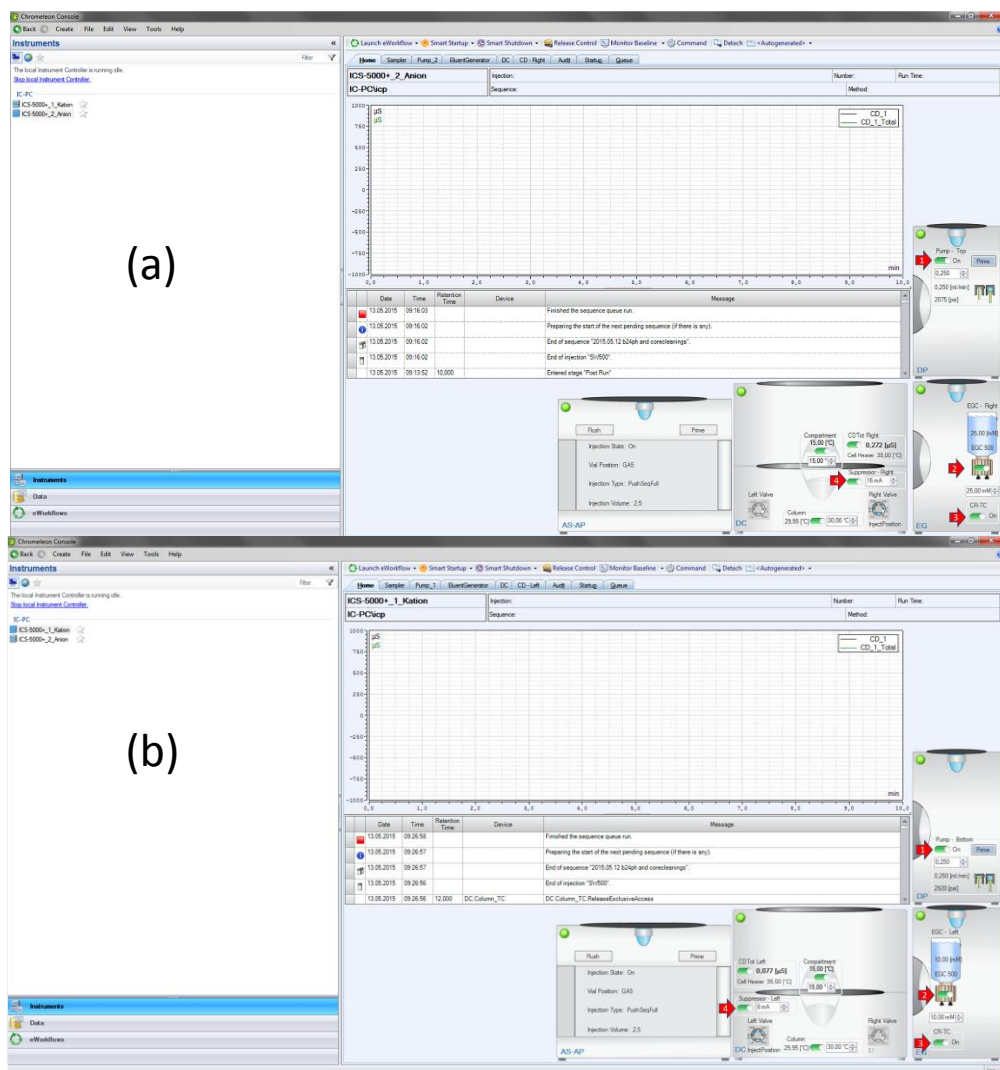


Figure A-5. Venting the air from pumps

6. Set pump parameter & turn on switch

For each Cation and Anion experiment, turn on pump by pressing switch 1 (marked by red arrow) and prime button respectively in the Figure A-6.



**Figure A-6. Preparing the instruments in the program of the IC software for (a) Anion and (b) Cation**

7. Set eluent concentration  
Specify eluent concentration for Cation and Anion experiment. For Anion experiment: 25mM (figure A-6 a). For Cation Experiment: 10 mM (figure A-6 b)
8. Set suppressor current  
Specify suppressor current for Cation and Anion experiment. For Anion experiment: 16 mA (figure A-6 a). For Cation Experiment: 8 mA (figure A-6 b)
9. Turn on switches, wait stable CD total  
Turn on switch 2, 3, and 4 (marked by blue arrow) respectively for each Cation and Anion experiment as shown in the figure above. After turning on the switches, wait until CD total ( $\mu\text{s}$ ) is stabilized. The stabilized value has to be checked with the previous values and recorded in the related note book

## 10. Start program

Add data file for each Cation and Anion experiment in the queue list. Then start the experiment by pressing start button (Figure A-7).

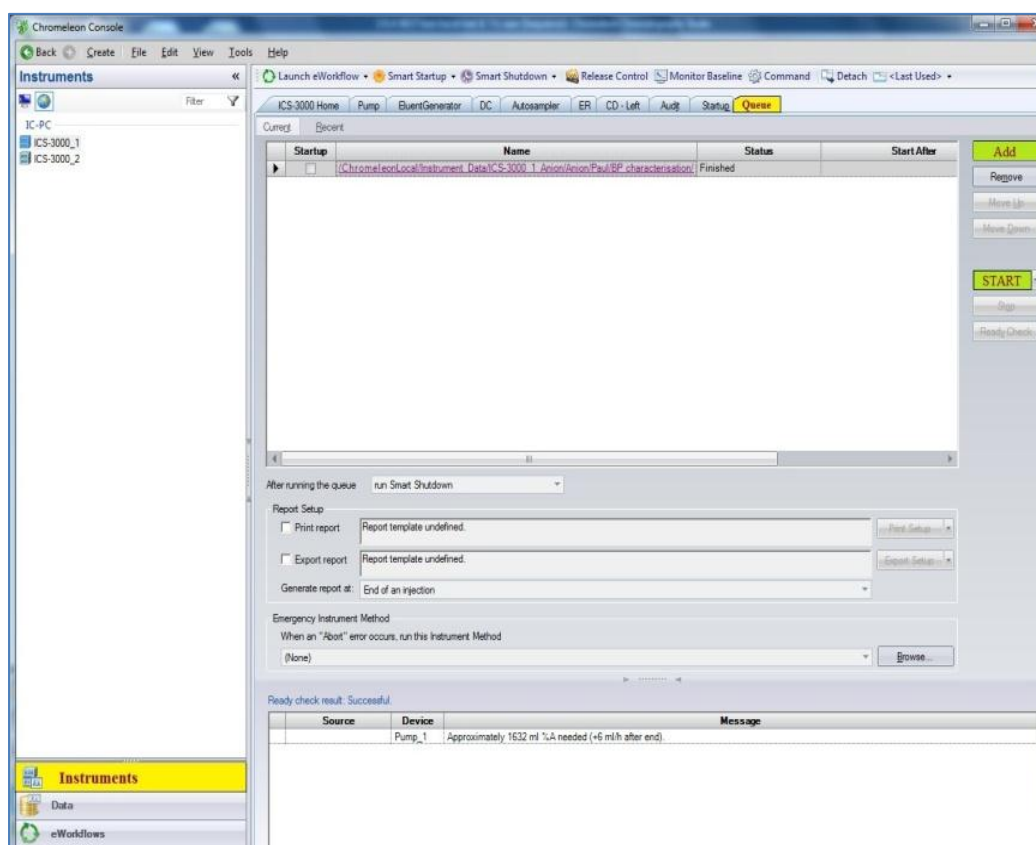


Figure A-7. Adding and starting the measurement in IC system

## 11. Analyze the result

The final step is analyze the result to get ion composition. Different ions show their conductivity peak in different intervals of retention time in the resin column. For example as shown in Figure A-8, the peak of calcium ion appears at about 7.3-11.5 min. First, the base lines for all the ions of the entire samples have to be corrected. Then the resulted areas ( $\mu\text{s} \cdot \text{min}$ ) of a specific ion in all the samples have to be transferred to concentration, based on the average area of the reference samples (which is normally diluted sea water).

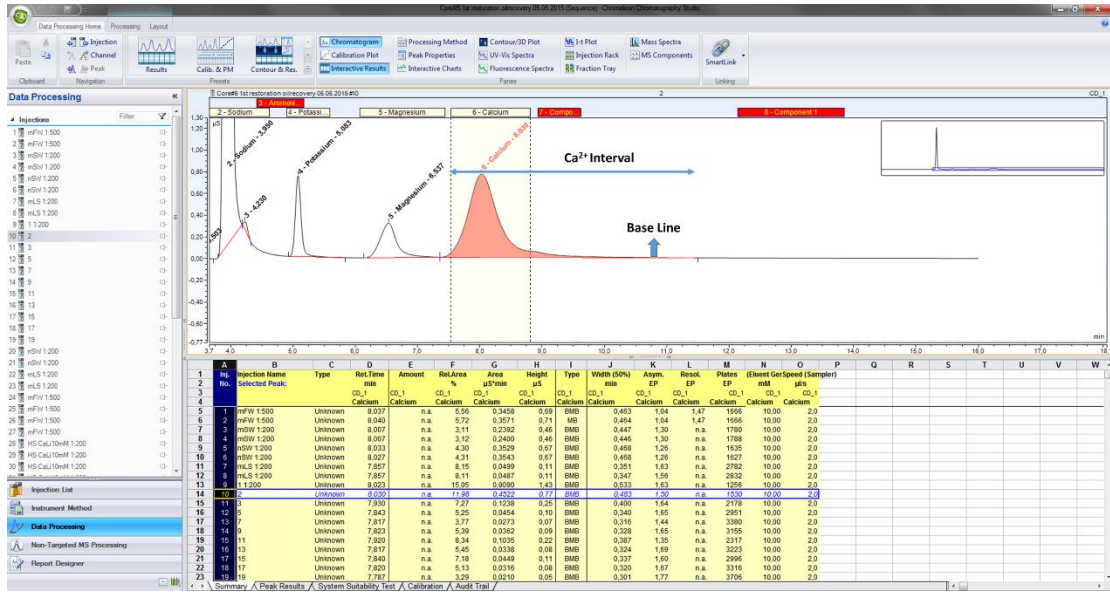


Figure A-8. Analyzing the obtained result after IC measurements